THEORETICAL STUDY OF MULTICYCLIC CONTROL OF A CONTROLLABLE TWIST ROTOR

PREFACE

The work performed on this contract was under the technical direction of John L. McCloud, III, NASA Ames Research Center, Moffett Field, California.

The authors wish to acknowledge the guidance and assistance provided by Mr. McCloud throughout the program and to thank him for his enthusiastic support. Especially useful were his technical contributions that provided better insight to establishing methods that define optimum multicyclic control mixes for improved performance and reduced vibration. A description of the methods developed at Ames is presented in Reference 1.

Financial support for the program was supplied by the U. S. Army Air Mobility Research and Development Laboratory, Ames Directorate.

TABLE OF CONTENTS

LIST OF ILLUSTRATIONS

LIST OF TABLES

INTRODUCTION

The sources, the problems, and the detrimental effects of high level, low frequency helicopter vibration are well known. The major sources of these vibrations are rotor induced shears and moments. Problems resulting from high vibrations increase the development time and cost of rotary-wing aircraft, are a source of pilot and crew fatigue, and are a primary cause of lower helicopter availability due to increased maintenance and reduced reliability of structure and equipment. The need for helicopter vibration reduction has long been recognized and has been sought for many years through research in rotor aeroelasticity to control the source, in structural dynamics to tune the structure, and in vibration mitigation devices to develop effective isolation and absorber systems.

One of the concepts with great potential for reducing hub shears and moments is a blade dual control system which controls the radial and azimuthal distribution of blade loading. The dual control system consists of a primary inboard pitch horn control and a secondary outboard flap control. The flap can be either mechanical as in the Kaman servo flap or aerodynamic, as in the jet flap.

In general, the secondary control will also disturb trim, altering the primary control settings required for any specified force trim condition. In contrast to a conventional rotor with a single, unique control setting required for a particular trim condition, a dual control rotor may be trimmed with a large number of possible control settings, some of which will be better than others. Trim control, therefore, becomes an optimization problem, with the objective of selecting input primary and secondary control settings to achieve a specified trim point at the most favorable trade-off of performance parameters.

In a study completed under contract to USAAMRDL, Eustis Directorate, and reported in Reference 2, Kaman evaluated the potential benefits of a dual control system. The concept studied is called Controllable Twist Rotor, or CTR. It combines two proven systems - conventional pitch horn controls and Kaman's servo flap - to optimize blade pitch, elastic twist, and airloads throughout a complete rotor revolution. It was found that the dual control concept was effective in reducing peak loadings and controlling harmonic load distribution. Improvements in performance, stall, compressibility and hub shear reduction are corollary.

Full scale tests of a rotor with jet-flaps on the outer 30 percent of the rotor blade were made by Giravions Dorand in the NASA Ames 40 ft x 80 ft wind tunnel. The results, reported in References 3 and 4, showed large reductions of rotor blade bending stresses when the jet-flaps were deflected multicyclically, i.e., with second, third, and fourth harmonic content. The vibratory loads transmitted to the fuselage were also reduced with no significant penalty in rotor performance. These results indicate a potential for similar vibration alleviation by simpler mechanical type servo flaps.

A more recent study, using the analytical results reported herein, examined various optimization schemes to establish the most effective mix of multicyclic flap controls for reduction of pylon vibratory loads and blade bending moments. The results of the study, reported in Reference 1, show virtual elimination of pylon vibratory loads occurring concurrently with blade bending moments that are reduced by 50 percent. Amplitude requirements for the higher harmonic flap deflections to attain these reductions are of the order of four degrees.

The analytical work reported herein covers the methods developed and used to calculate the airloads and responses of a dual control rotor system with multicyclic flap controls. Special analyses to trim the dual control rotor for level flight are discussed and techniques are developed which sequentially search trimmed flight conditions and select control combinations that result in optimized operational characteristics. A range of rotor disk loadings is examined at a prespecified flight condition to evaluate multicyclic control flap effectiveness.

ANALYTICAL METHODS

ROTOR AEROELASTIC ANALYSIS

As part of the CTR study of Reference 2, Kaman developed an aeroelastic computer analysis to "fly" a CTR system throughout various flight conditions. The equations of motion in the aeroelastic analysis couple six response modes and two control modes for a fully articulated rotor system. The response modes include blade pitching, lagging, flapping, flapwise bending, twisting, and servo flap pitching. The dual controls include swashplates which drive a pitch horn at the blade root and a servo flap near the blade tip. Figures 1 and 2 illustrate the controls and the assumed displacements used in the analysis.

The modal approach is used to evaluate the airloads by mathematically describing blade motions with the listed six degrees of freedom. The complete inertial and centrifugal terms for the equations of motion are derived through the use of matrix transformations. Potential strain energy and dissipative energy terms are included in the equations of motion by assuming concentrated springs and viscous dampers for the four rigid body modes, and by evaluating the fundamental bending and torsional frequencies of the rotating blade for the flapwise and torsion modes.

Generalized aerodynamic forces for each of the six modes are obtained from strip theory by calculating an instantaneous local airfoil section Mach number and angle of attack and using these to evaluate aerodynamic force coefficients from available wind tunnel data. In the mechanical flap region, additional secondary control effects are computed and added to the blade dynamics. In their present form, the aeroelastic equations of motion include all nonlinear inertial coupling effects and nonlinear aerodynamic effects such as reverse flow, stall, Mach number variations, large induced flow angles, and variable inflow. Additional features to the analysis are the inclusion of feedback mechanical coupling among the flap, blade feathering, blade flapping, and blade lagging motions and the inclusion of arbitrary spring rates and dampers for each mode. Any one or combination of these parameters can be eliminated easily from the analysis. Furthermore, spring rates for the two types of control system are also included in order that accurate control loads can be calculated. A flow chart of the computer program is shown in Figure 3. The detailed equations of motion and the numerical methods of solution are presented in References 2 and 5.

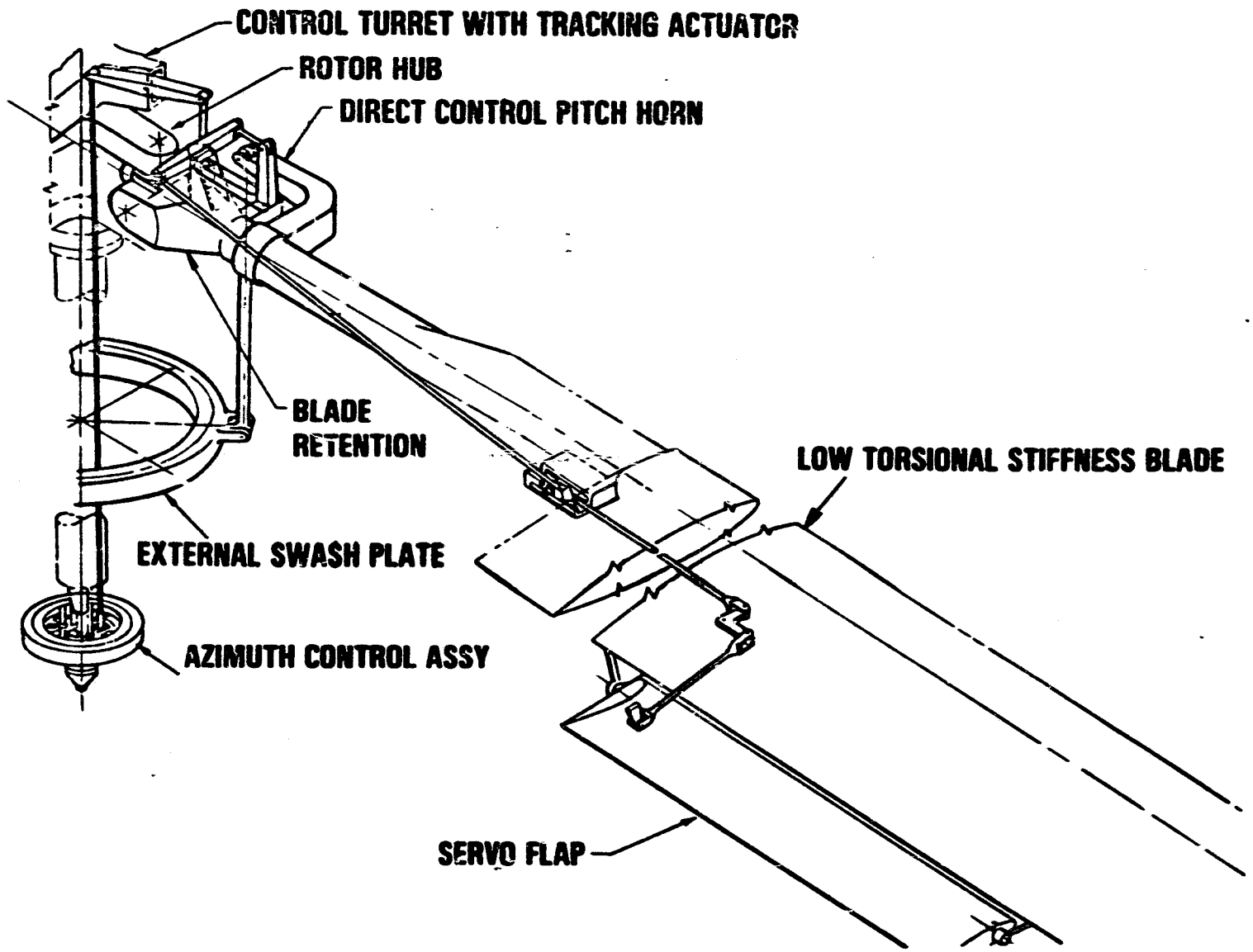

Figure 1. Control Arrangement for Controllable Twist Rotor (CTR).

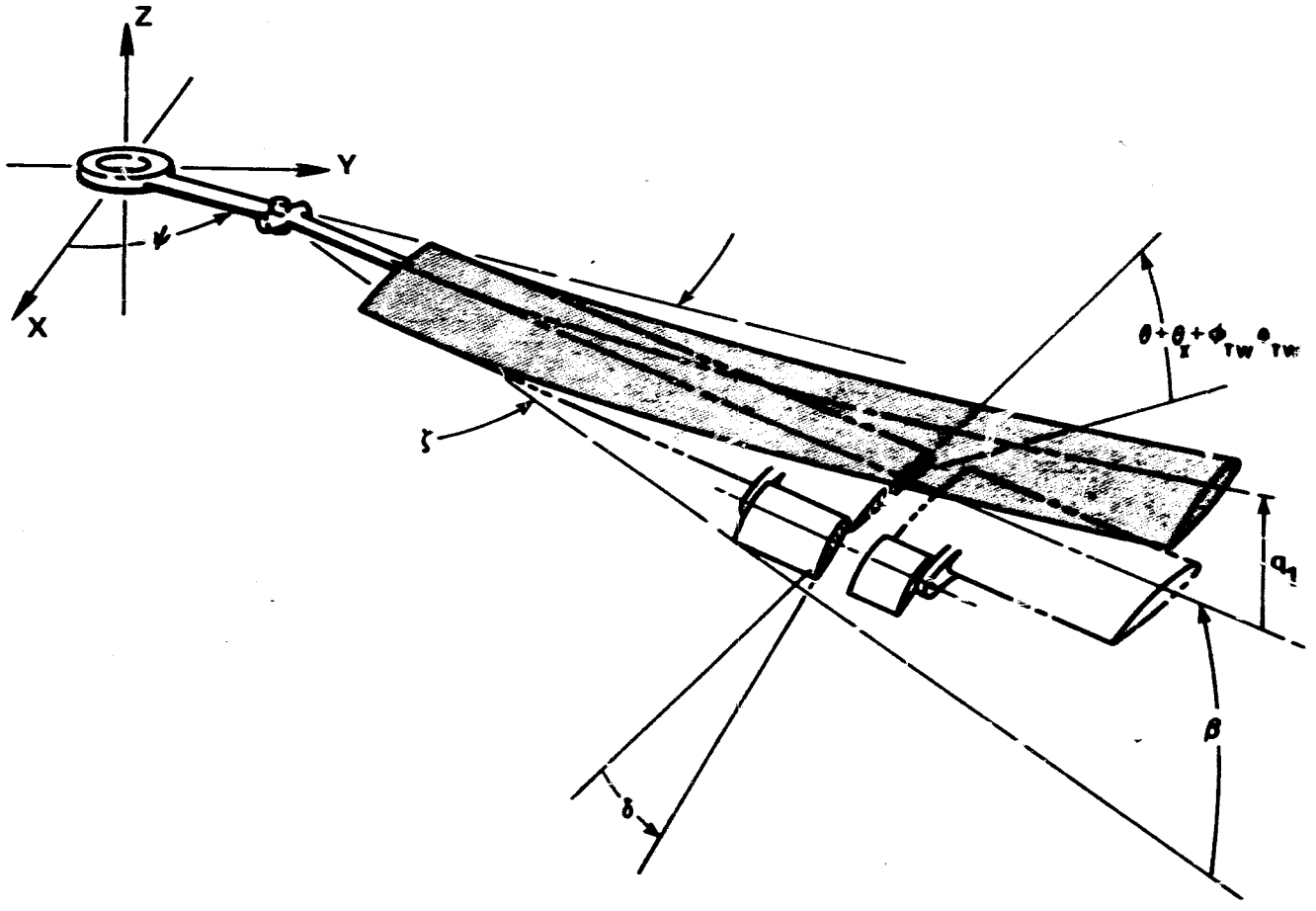

Figure 2. Controllable Twist Rotor Displacements.

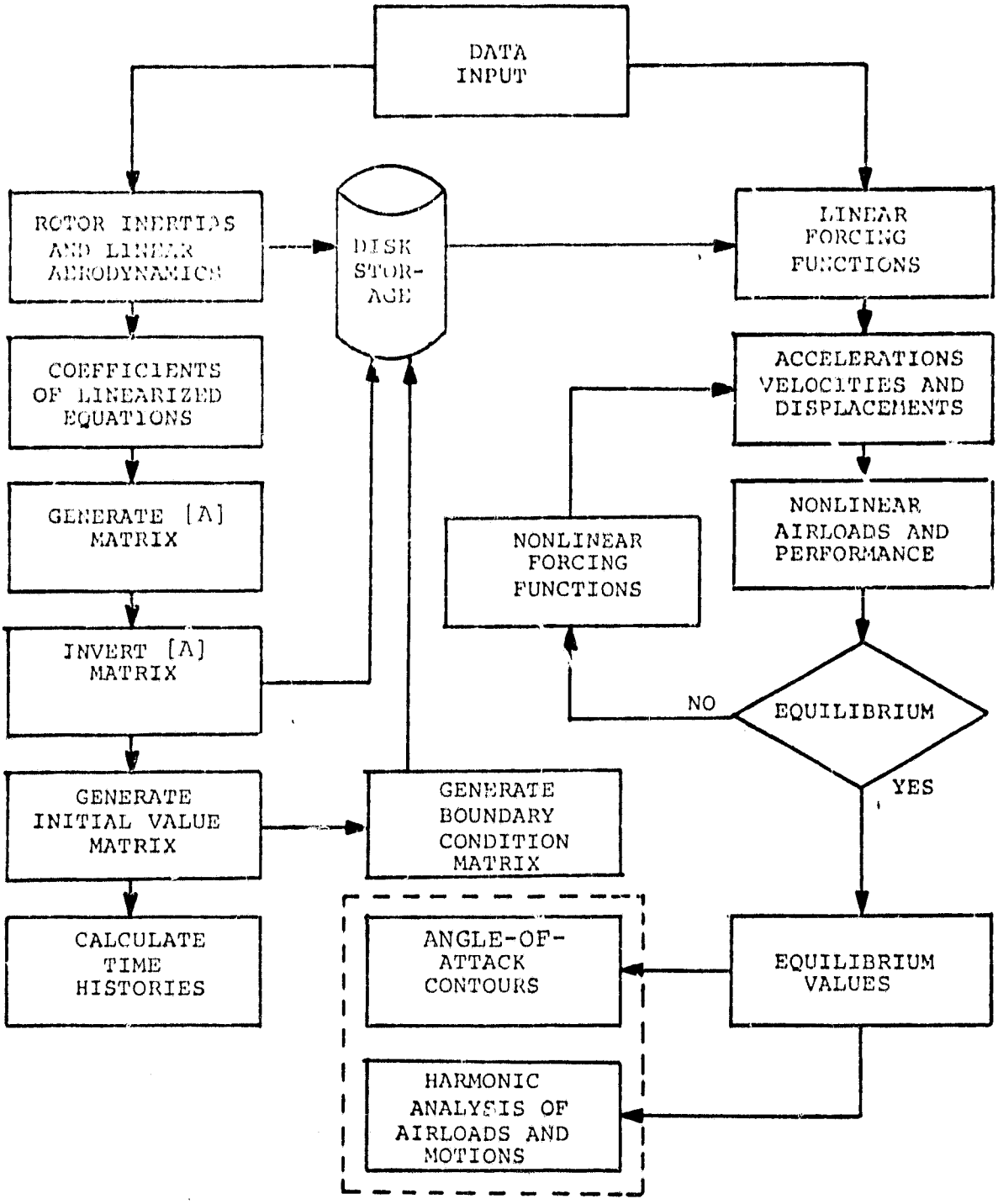

Figure 3. Flow Chart of the Computer Program for the Controllable Twist Rotor (CTR) Theoretical Analysis.

ROTOR TRIM CONSIDERATIONS

It has long been recognized in the helicopter industry that comparisons between rotor systems are valid only when two systems are trimmed to the same integrated hub forces and moments. This is particularly true when the items of interest are airloads, stresses, and root shears. Attempts to suppress vibrations through higher harmonic inputs are especially sensitive in this regard.

A rotor system with a single control input has a unique combination of collective and cyclic control values which generates the required hub trim forces at a specified speed. The trim provisions common to all analyses in the industry are designed to home in on the unique combination appropriate to that flight condition. However, as shown in Figure 4, simultaneous collective, cyclic, and higher harmonic controls can be input to the pitch horn and to the servo flap of a controllable twist rotor. Thus, a dual control rotor system has many combinations of collective and cyclic inputs which will result in the same trim forces. The CTR analysis automatically changes the collective and cyclic controls until the rotor is trimmed to a prespecified flight condition. The computer program has been configured so that it simulates CTR systems with multicyclic control for a wide variety of aircraft.

Optimizing dual controls involves a procedure which requires calculation of several trim conditions and, therefore, several times as many trimmed computer runs as is normally required for a conventional single control rotor. This is true even when the secondary control is used primarily for vibration suppression. A separate optimization analysis supplements the aeroelastic airloads and trim program. The optimization analysis generates response surfaces as functions of the independent control parameters and uses steepest descent techniques to select the combination of these parameters that optimizes the desired dependent variables. For example, the response surfaces are used to estimate control inputs which maximize performance and minimize blade dynamic response. To complete the procedure, these estimated optimum control inputs are then used to generate new trimmed optimum flight conditions for the dual controlled rotor through use of the aeroelastic loads analysis. The specific equations that are used to generate the response surfaces are presented in the section of this report entitled OPTIMIZATION TECHNIQUES.

VARIABLE INFLOW MODEL

Historically, three major approaches to modeling the non-uniform flow field of a helicopter rotor have been used by the industry. The least expensive, least accurate, and least complex approach is uniform inflow. In this approach, the flow field has a uniform velocity through the rotor, at a value determined by using the specified value of thrust coefficient and momentum theory. Such an approach is inadequate for this study because of the lack of harmonic content, whose interactions with the multicyclic flap are expected to be an important effect in the final conclusions reached.

TRIM ANALYSIS

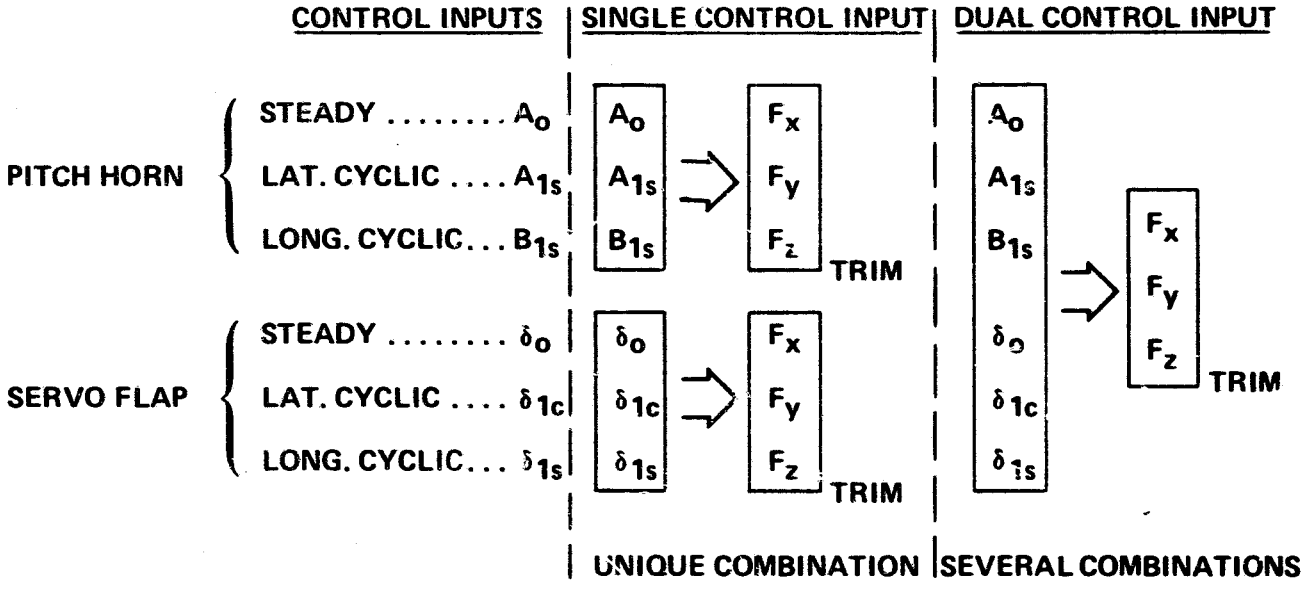

Figure 4. Control Input Combination for Rotor Trim.

The most expensive, most complex, and most detailed approach is the so-called Free Wake or Flexible Wake method including its later developments such as Distorted Free Wake. In this approach, the interactions of the trailed vortices are included while determining their locations in space and time. They are then superimposed to obtain the flow field values at the rotor. Disadvantages of this method are its high cost and its oversensitivity. This method is sensitive to higher harmonics of tip path plane warping and blade bending deformations, and uses extensive matrix operations. As a result, it is possible to compute inflow values at intermediate steps of a trim iteration which causes a mathematical divergence of the iteration. The additional complexity of each case and the added cases implied by the artificial trim divergence combine to increase significantly the cost of the method.

An intermediate method in terms of cost, complexity, and accuracy is the Prescribed Wake Method (Rigid Wake). In this approach, the vortex wake is considered to be convected from the rotor by momentum considerations, and only the influence of the near wake on the flow field at the rotor is computed. The "nearness" of the near wake depends on choice of the user - it is usually described in terms of rotor revolutions. The wake model itself is a set of trailed vortices, ranging to as many as ten, although four is usually an adequate number. Because the location of the wake in this method is primarily a function of advance ratio and thrust coefficient, the inflow model is relatively insensitive to the excursions one goes through while trimming a rotor. Furthermore, because the inflow model remains constant during the trim process, two major discomforts are avoided. First, one need not be concerned with whether the wake model will be consistent with the cyclic/collective pitch control input combination or with the cyclic/collective/flap control input combination eventually reached at trim. By definition, the wake model will be consistent with the control combinations at trim. Second, the absence of mathematical instabilities arising from the wake model/trim model interactions assures that trim iterations will not diverge because of inflow problems.

Because a large number of cases is required to determine the proper multicyclic flap system parameters to minimize vibrations and because each of these cases must represent trimmed flight conditions, the cost savings of the Prescribed Wake method are significant. As for accuracy, it is important to note that the velocities at which a vibration suppressant control flap would be most desirable (115 knots and above) match the range over which the Prescribed and Free Wake methods agree closely for a trimmed vehicle. For these reasons, the Prescribed Wake Method was used in the analysis reported herein.

RANGE OF STUDY

The primary purpose of the multicyclic flap system is to reduce helicopter vibration levels by reducing rotor generated vibratory loads that are transmitted to the fuselage. Although vibration problems are more severe at extreme operating conditions, the accurate prediction of rotor loads and performance at those conditions is difficult. Therefore, the prime thrust of this investigation is in areas where retreating blade stall and high advancing blade Mach number effects are not significant. Rotor blade and disk loadings correspond to contemporary practice, and the propulsive force is representative of utility type helicopters.

In consonance with the preceding discussion, the following flight conditions and loading conditions were investigated for the CTR with multicyclic controls.

Advance Ratio:	.333
Disk Loading:	4.75 to 5.5 psf
C_z/σ:	.090 to .106
C_x/σ:	.0071

The preceding parameters correspond to a rotor that has a diameter of 56 feet, a tip speed of 613 fps, and a solidity of 0.062. The ranges of disk loading, blade loading, and propulsive force loading correspond to the sea level flight conditions of a utility helicopter with a gross weight range of 11,500 to 13,500 pounds and a flat plate drag area of 20 square feet. The study was conducted at an advance ratio of 0.333 which corresponds to 120 knots.

Figures 5 to 7 show the planform, inertia and stiffness characteristics of the rotor used in this study. The study used existing CTR design which was based on an H43 helicopter blade configuration, circa 1950, hence English units were used throughout the study.

The physical span of the servo flap considered for this study was 36 inches. In order to account for the finite aspect ratio of the flap and its attendant vortex tip losses, the servo flap was modelled to have a span of 24.5 inches with 5.75 inch linear taper at each end thereby resulting in a trapezoidal planform. This planform modelling is shown in Figure 5.

Inboard of Station 100, the blade transitions from an airfoil cross-section to a rectangular cross-section which is fitted with a root end grip. Because of this transition, the twist distribution is highly nonlinear in this region. The geometric twist distribution corresponding to these inboard blade stations is shown in Figure 6.

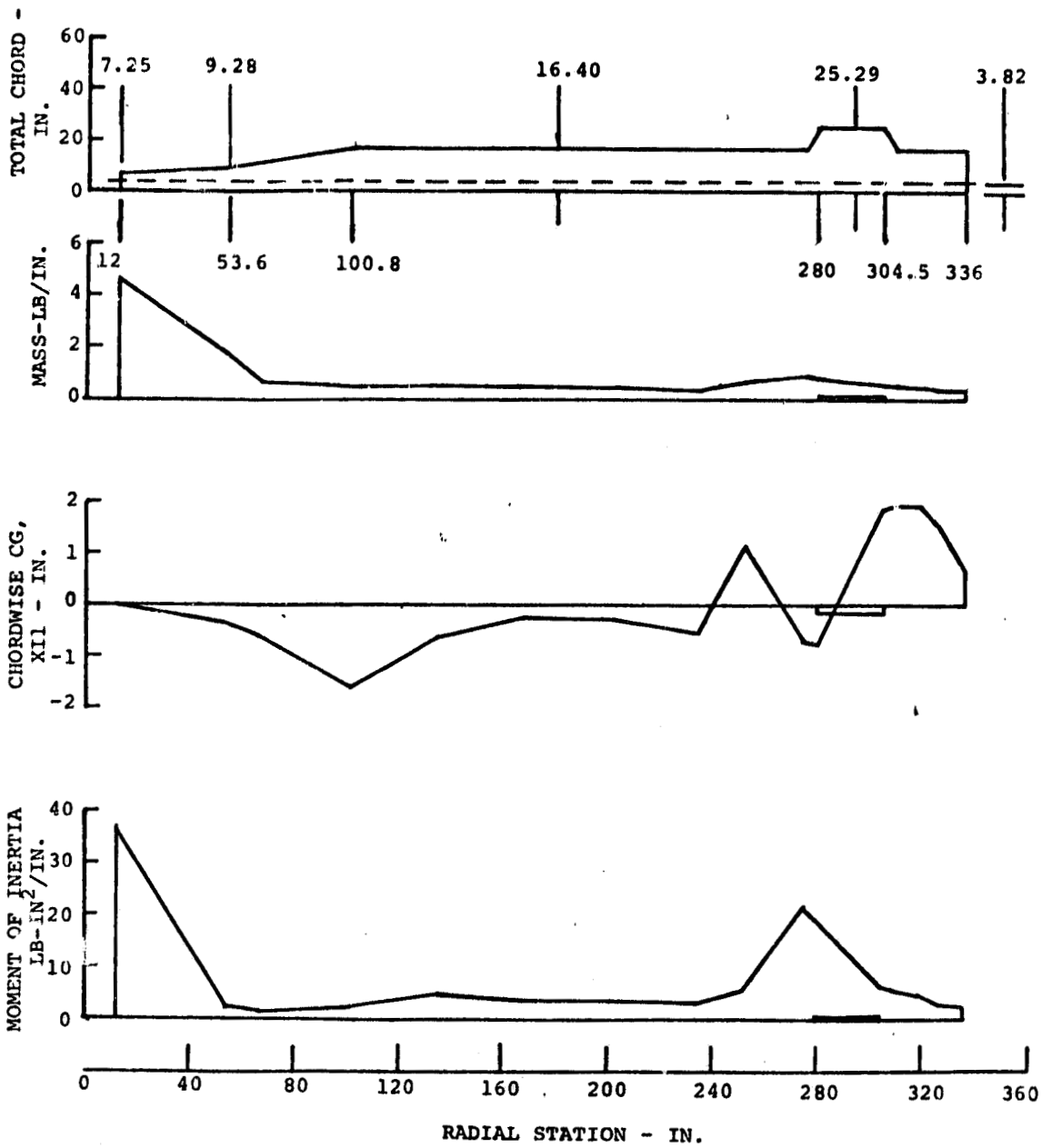

Figure 5. Rotor Blade Planform and Inertia Characteristics.

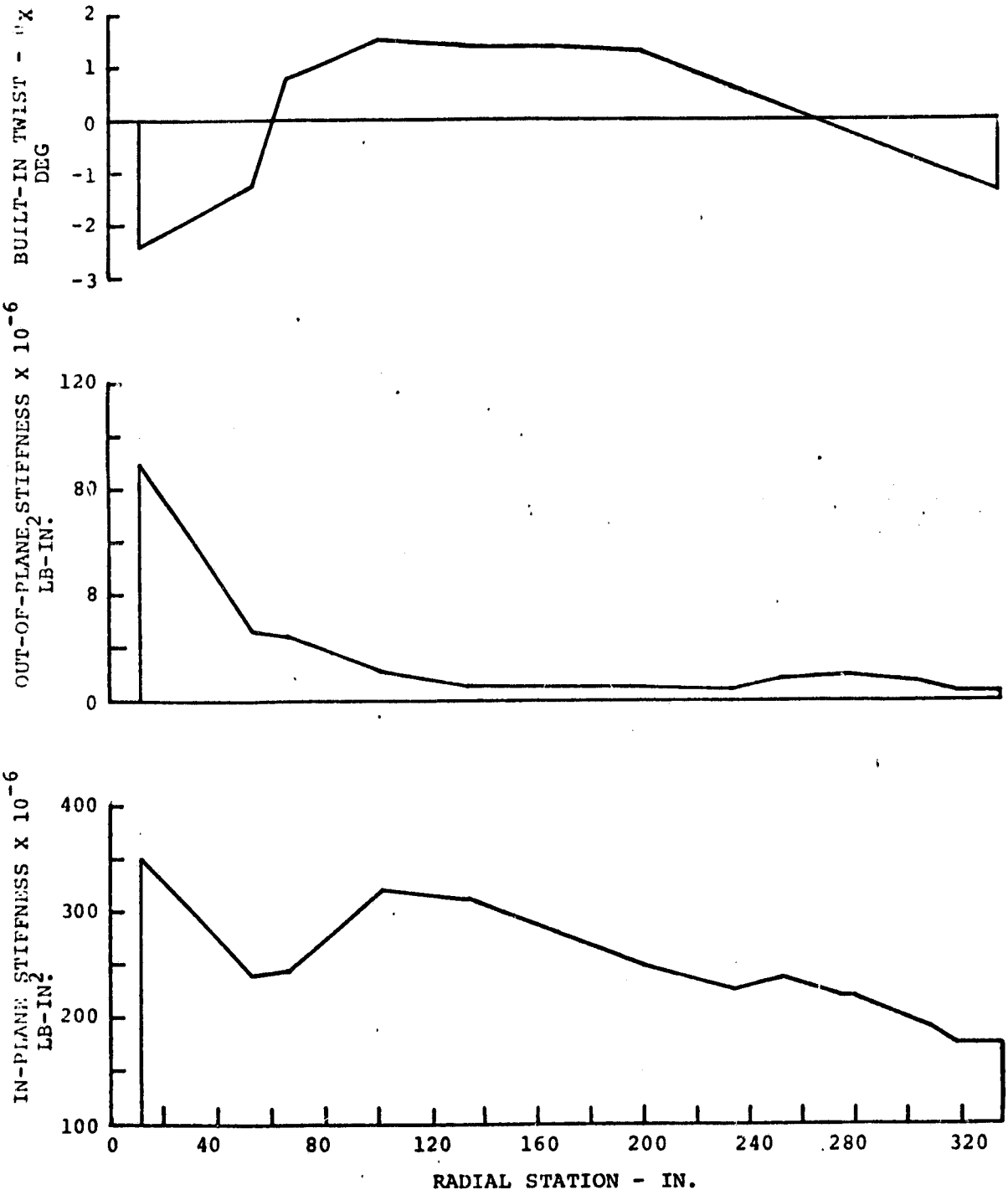

Figure 6. Rotor Blade Twist and Stiffness Characteristics.

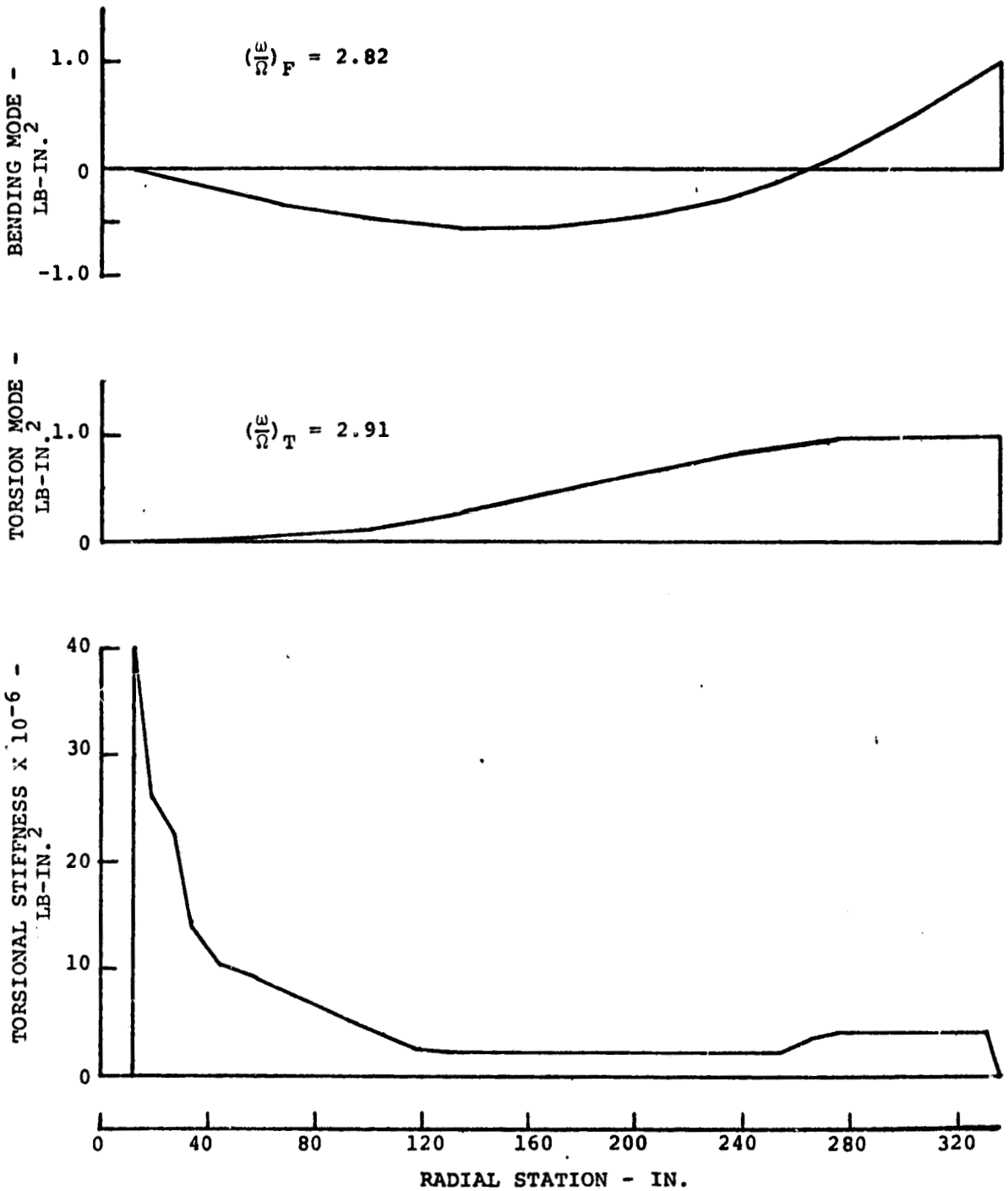

Figure 7. Rotor Blade Stiffness and Mode Shape Characteristics.

OPTIMIZATION TECHNIQUES

ANALYTICAL PROCEDURE

CTR (First Harmonic Flap)

For the preliminary phase of this study (baseline CTR cases), three disk loadings were investigated with constant inflow across the disk (λ = -.037). The rotor drag C_x/σ was held constant for all three rotor lifts investigated, at .0071. A number of cases were repeated with a variable inflow that averaged -.037 across the disk with negligible effect on trim.

As outlined previously the initial step in dual control optimization is to select the control range of the secondary control and design a control matrix to provide the maximum information about the performance parameters. Shown in Figures 8 through 10 are the flap control matrices selected as starting points. These collective and first harmonic flap inputs were felt to bracket the probable range of acceptable flap travel to trim. This basic schedule could be modified if trim could not be attained or the resulting information indicated the data was in an unacceptable area such as stall regime. Use of data from extreme cases would prejudice the results of the regression model. For the first harmonic flap study, the following rotor parameters were used as a measure of the effectiveness of the secondary control:

(a) Rotor horsepower.

(b) Maximum local blade angle of attack.

(c) Maximum vibratory out-of-plane bending moment.

(d) Vibratory pylon excitation (four/rev).

(e) Number of iterations to converge.

The maximum local blade angle of attack was selected between blade normalized station of .50 to .97 as this area would not be affected by reverse flow region. The number of iterations to converge was felt to be a measure of blade stability - fewer iterations to converge the more stable the blade configuration.

Since this is a four-bladed rotor, the root shears can be resolved in 4/rev pylon excitation in the fixed reference system by the following transformations:

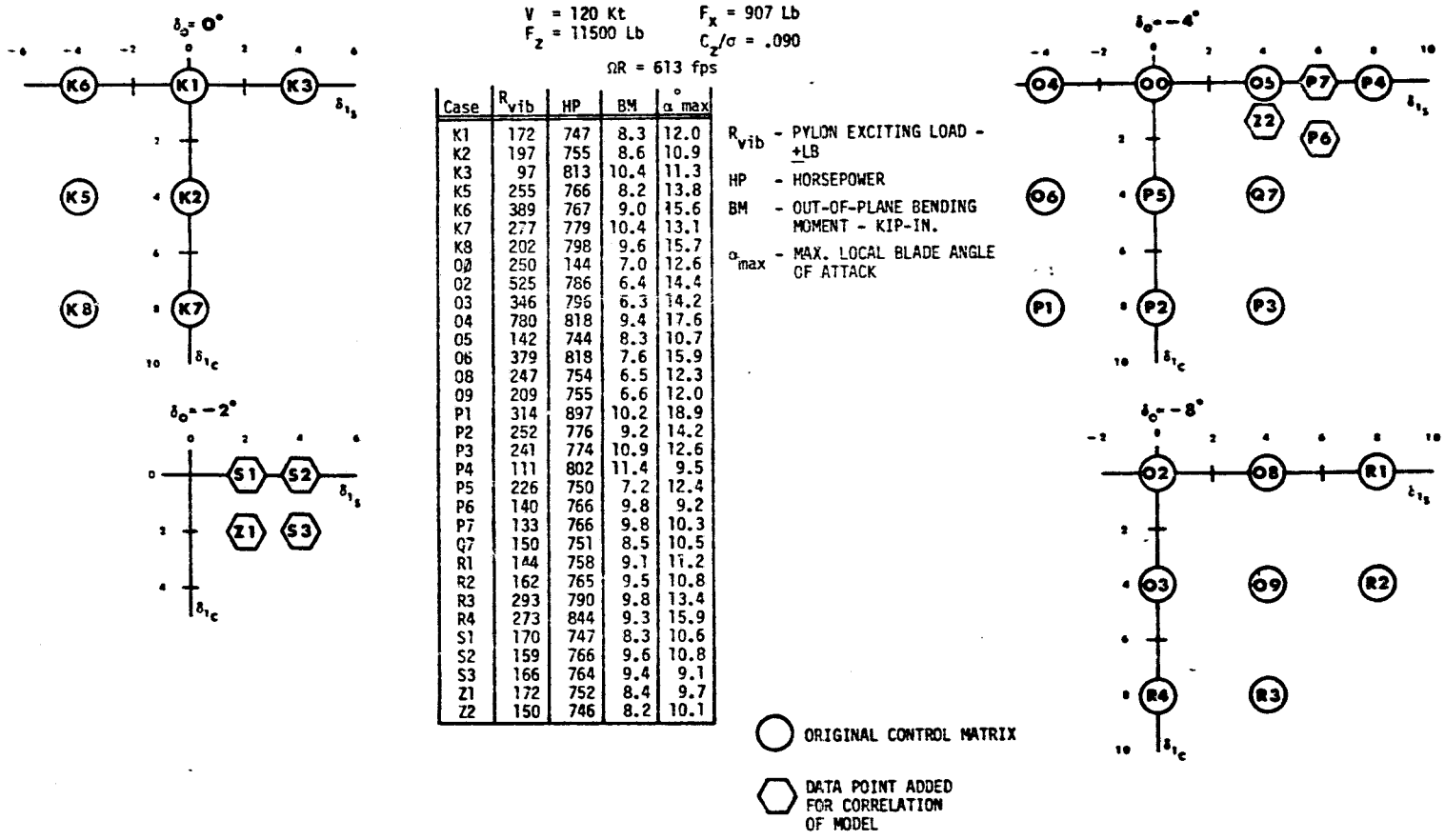

Case	R_{vib}	HP	BM	α_{max}
K1	172	747	8.3	12.0
K2	197	755	8.6	10.9
K3	97	813	10.4	11.3
K5	255	766	8.2	13.8
K6	389	767	9.0	15.6
K7	277	779	10.4	13.1
K8	202	798	9.6	15.7
OØ	250	144	7.0	12.6
O2	525	786	6.4	14.4
O3	346	796	6.3	14.2
O4	780	818	9.4	17.6
O5	142	744	8.3	10.7
O6	379	818	7.6	15.9
O8	247	754	6.5	12.3
O9	209	755	6.6	12.0
P1	314	897	10.2	18.9
P2	252	776	9.2	14.2
P3	241	774	10.9	12.6
P4	111	802	11.4	9.5
P5	226	750	7.2	12.4
P6	140	766	9.8	9.2
P7	133	766	9.8	10.3
Q7	150	751	8.5	10.5
R1	144	758	9.1	11.2
R2	162	765	9.5	10.8
R3	293	790	9.8	13.4
R4	273	844	9.3	15.9
S1	170	747	8.3	10.6
S2	159	766	9.6	10.8
S3	166	764	9.4	9.1
Z1	172	752	8.4	9.7
Z2	150	746	8.2	10.1

Figure 8. CTR Control Matrix, GW = 11500 Lb.

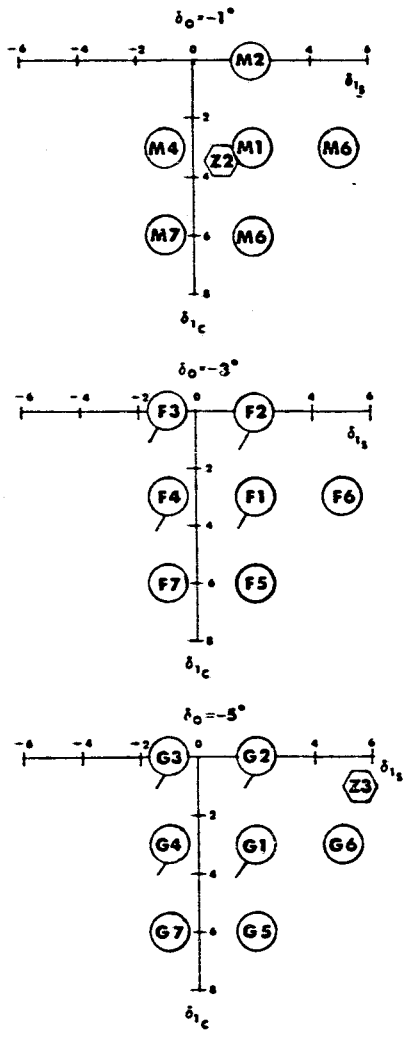

CTR CONTROL MATRIX

V = 120 Kt F_x = 907 Lb
F_z = 12500 Lb C_z/σ = .098
ΩR = 613 fps

Case	R_{vib}	HP	BM	$\alpha°_{max}$
F1	215	787	7.9	11.7
F2	232	787	8.4	12.8
F3	539	817	9.3	15.3
F4	370	814	7.9	13.7
F5	237	799	8.1	12.8
F6	184	795	9.8	10.5
F7	264	826	8.3	11.9
G1	278	794	7.3	12.9
G2	332	790	7.9	13.3
G3	902	866	10.5	17.2
G4	494	848	7.9	15.1
G5	262	815	7.6	13.6
G6	192	788	8.5	11.3
G7	347	877	8.4	16.3
K1	381	824	7.0	13.9
K5	325	843	8.3	14.6
M1	211	795	8.9	10.9
M2	222	792	9.2	12.6
M4	258	789	8.1	12.6
M5	240	792	8.7	12.2
M6	208	794	11.2	9.8
M7	257	799	8.6	13.8
Z1	197	786	9.1	11.0
Z2	218	784	8.4	11.6
Z3	193	782	9.1	11.4
Z4	216	786	9.2	10.9
Z5	280	807	10.1	19.8
Z6	197	802	9.9	12.0
Z7	174	769	8.6	10.8
Z8	196	785	8.8	11.2
Z9	198	787	9.8	10.8

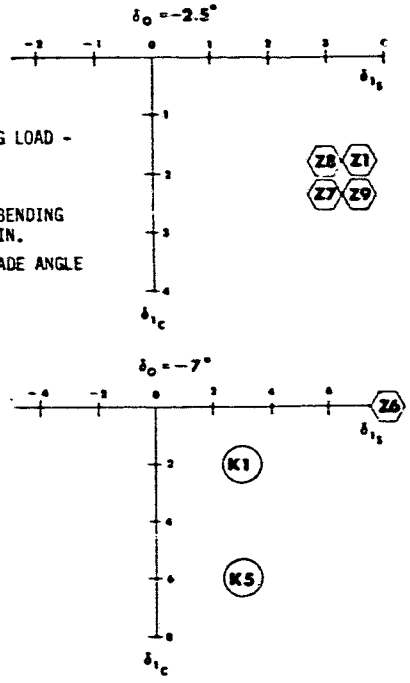

R_{vib} - PYLON EXCITING LOAD - ±LB
HP - HORSEPOWER
BM - OUT-OF-PLANE BENDING MOMENT - KIP-IN.
α_{max} - MAX. LOCAL BLADE ANGLE OF ATTACK

NOT PLOTTED: δ_o = 0°; δ_{1s} = 1.5°; δ_{1c} = 3°
NOT PLOTTED: δ_o = 3°; δ_{1s} = -2°; δ_{1c} = 0

ORIGINAL CONTROL MATRIX

CASE FOR PRELIMINARY MODEL

DATA POINT ADDED FOR CORRELATION OF MODEL

Figure 9. CTR Control Matrix, GW = 12500 Lb.

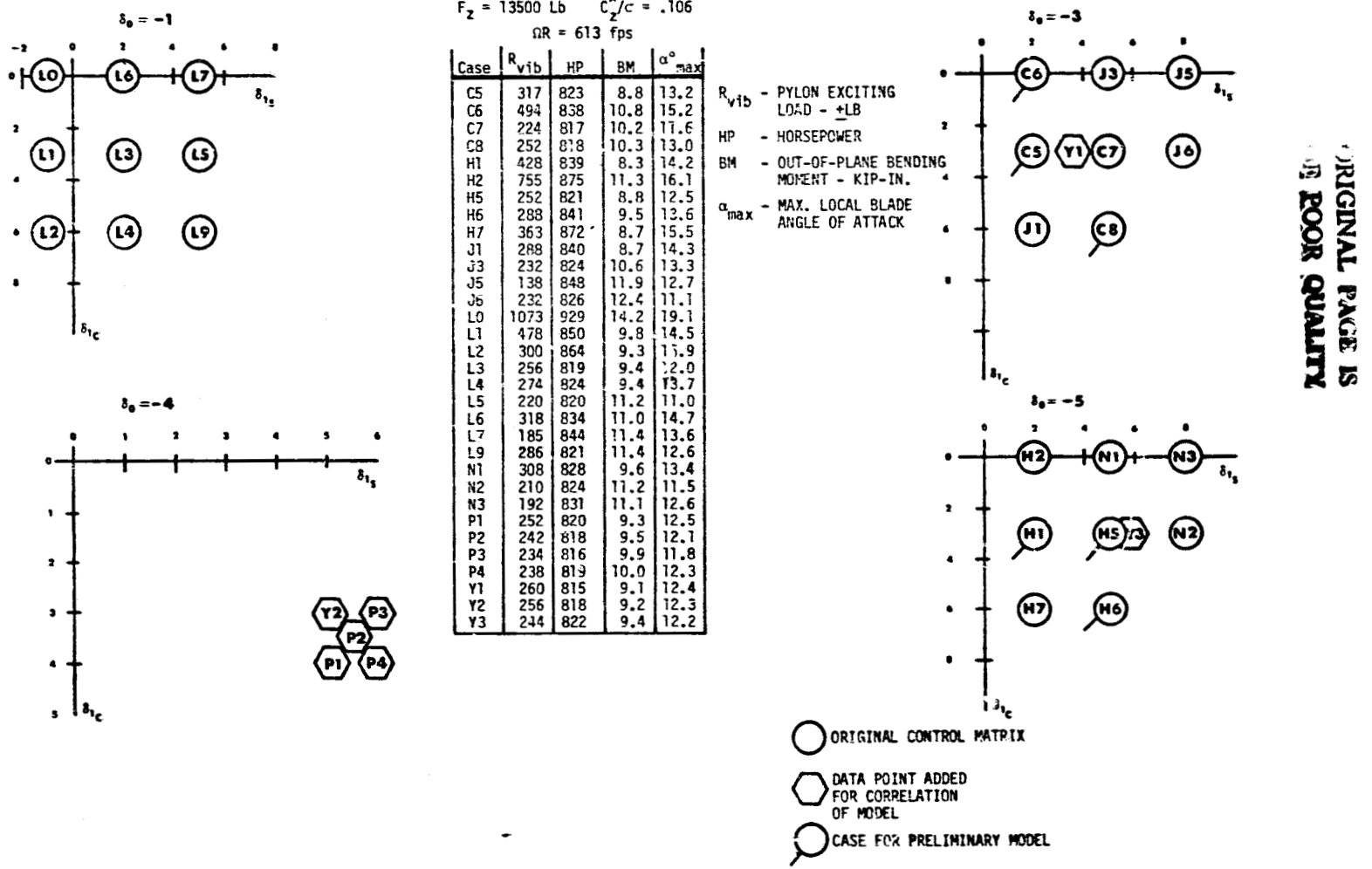

Case	R_{vib}	HP	BM	$\alpha°_{max}$
C5	317	823	8.8	13.2
C6	494	838	10.8	15.2
C7	224	817	10.2	11.6
C8	252	818	10.3	13.0
H1	428	839	8.3	14.2
H2	755	875	11.3	16.1
H5	252	821	8.8	12.5
H6	288	841	9.5	13.6
H7	363	872	8.7	15.5
J1	288	840	8.7	14.3
J3	232	824	10.6	13.3
J5	138	848	11.9	12.7
J6	232	826	12.4	11.1
L0	1073	929	14.2	19.1
L1	478	850	9.8	14.5
L2	300	864	9.3	13.9
L3	256	819	9.4	12.0
L4	274	824	9.4	13.7
L5	220	820	11.2	11.0
L6	318	834	11.0	14.7
L7	185	844	11.4	13.6
L9	286	821	11.4	12.6
N1	308	828	9.6	13.4
N2	210	824	11.2	11.5
N3	192	831	11.1	12.6
P1	252	820	9.3	12.5
P2	242	818	9.5	12.1
P3	234	816	9.9	11.8
P4	238	819	10.0	12.3
Y1	260	815	9.1	12.4
Y2	256	818	9.2	12.3
Y3	244	822	9.4	12.2

Figure 10. CTR Control Matrix, GW = 13500 Lb.

Vertical

$$F_Z = 4a_4 \cos 4\psi + 4b_4 \sin 4\psi$$

Fore and Aft

$$F_X = 2(c_3 - c_5) \sin 4\psi + 2(d_5 - d_3) \cos 4\psi$$

Lateral

$$F_Y = 2(c_3 + c_5) \cos 4\psi + 2(d_3 + d_5) \sin 4\psi$$

The coefficients a and b are the out-of-plane cosine and sine components with c and d being the in-plane cosine and sine components respectively. The subscripts refer to the harmonic number of the root shear in the harmonic analysis.

A BASIC language program for the Hewlett-Packard HP 2000 performs these transforms and calculates the peak values per cycle for F_Z, F_X, F_Y, the in-plane resultant and the 3D resultant. (Appendix A)

Each of the four dependent variables outlined above can be expressed in quadratic form in terms of the independent control variables. These equations have constant coefficients and are developed for trim conditions only. Equation (1) is the typical form of the relationship between horsepower and the collective and first harmonic flap inputs used in the CTR portion of this study.

$$\begin{aligned} HP = {} & a_o + a_1\delta_o + a_2\delta_{1s} + a_3\delta_{1c} + a_4\delta_o^2 + a_5\delta_{1s}^2 \\ & + a_6\delta_{1c}^2 + a_7\delta_o\delta_{1s} + a_8\delta_o\delta_{1c} + a_9\delta_{1s}\delta_{1c} \\ & + a_{10}\delta_o\delta_{1s}\delta_{1c} \end{aligned} \qquad (1)$$

Similar equations were written for the remaining three parameters of interest. In order to define the coefficients of these equations, a minimum of eleven trimmed cases are required. These cases must be selected to include variations of each parameter to provide statistical degrees of freedom. A regression analysis of each data set is used to obtain the coefficients of each of the equations. Additional trim case data sets are used to provide better statistical correlation through the use of the regression analysis. Once the functional relationship is established for the dependent variables, the resulting equations can be used to conduct a parametric study. The three components of the pitch horn controls are also modeled and the predicted control positions are

used as input for the aeroelastic trim program. Appendix B is a listing of the regression analysis program SURGEN. The program uses a number of trim cases to calculate the rotor parameter equation coefficients for each disk loading desired. In addition, the multiple correlation coefficients, standard error of the estimate, and a table of residuals are listed by SURGEN. Analysis of residuals for sum, sum of squares, mean, variance and standard deviation and a listing of the orders of the residuals from the most negative to most positive are also tabulated for convenience.

Once the preliminary models are obtained, the next function is to conduct a trade-off study that will establish a region of flap control that would produce values of the five rotor parameters that meet the criteria established. This was accomplished by devising a plot program on the Hewlett-Packard computer that generates the representative contour plots of Figures 11 to 13. The shaded area of each of these figures represents the cyclic flap control regions which the models predict will insure all rotor parameters are within a prescribed range.

For the three flap collective settings shown, it appears that operation at -4 degrees of flap collective would permit the largest range of first harmonic input to the rotor for trim and still maintain the boundary conditions selected at this gross weight and forward speed. This is shown graphically by the larger shaded area included within all rotor parameter contours.

With the boundaries established by the models, the next step is to determine the degree of correlation between the models and the actual trim. This is achieved by running additional selective cases and using the results for comparison and to upgrade the model. This procedure can be repeated until satisfactory correlation is obtained. This procedure was utilized at all three load levels with some innovations being incorporated based on the experience gained from previous trials.

As the rotor lift was increased the maximum allowable values of our selected rotor parameters were reviewed to reflect the increased disk loading.

Multicyclic Flap Input

In the study of multicyclic control input, two gross weights corresponding to C_z/σ of .090 and .098 were investigated with the emphasis on the lower disk loading. The variable inflow option of the aeroelastic trim program was exercised; for C_z/σ of .090 the average inflow across the disk was -.037 with -.0392 being the average for C_z/σ = .098. A representative inflow distribution (C_z/σ = .098) is listed azimuthally and by blade radial station in Appendix C.

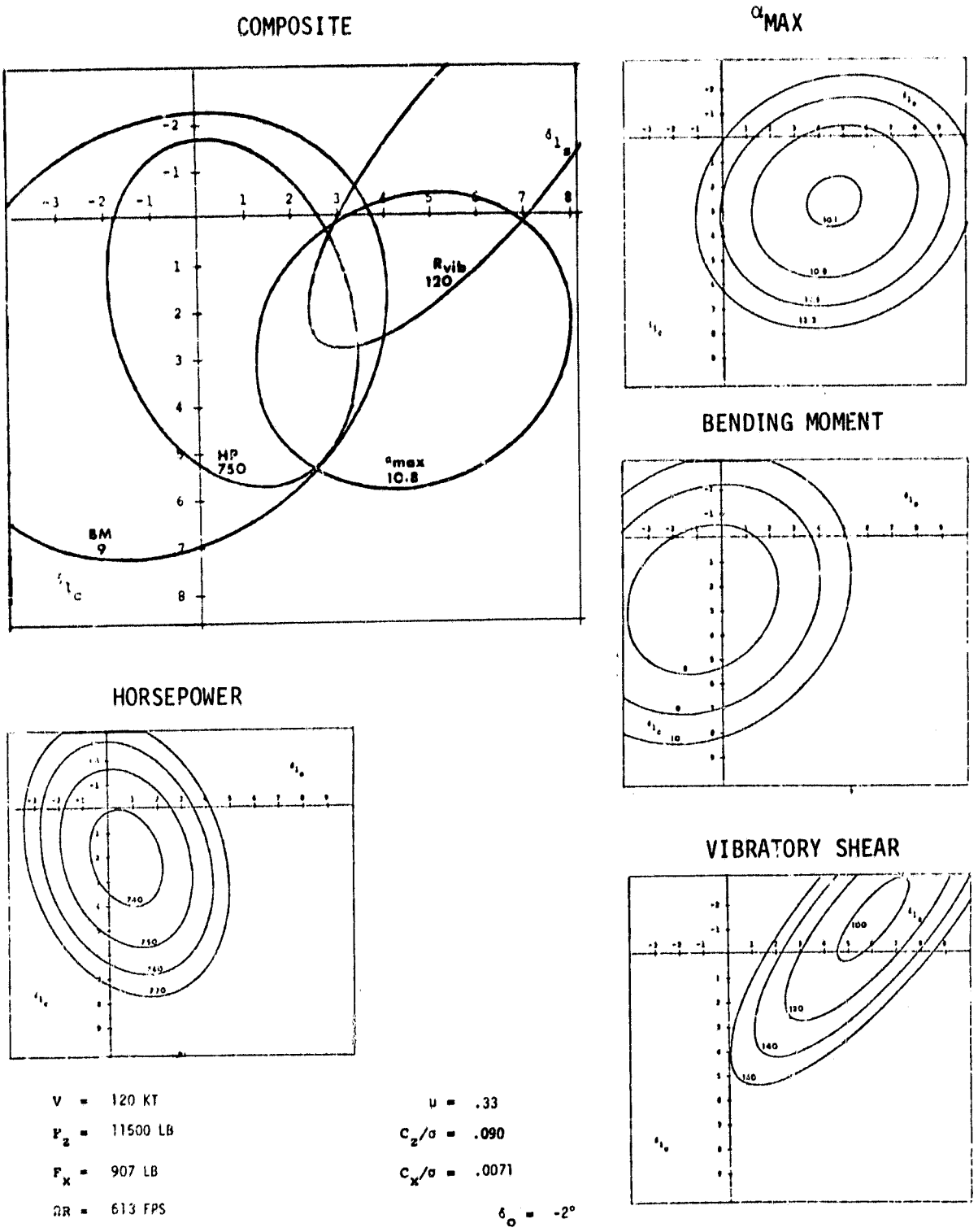

Figure 11. CTR Control Optimization, $\delta_o = -2°$.

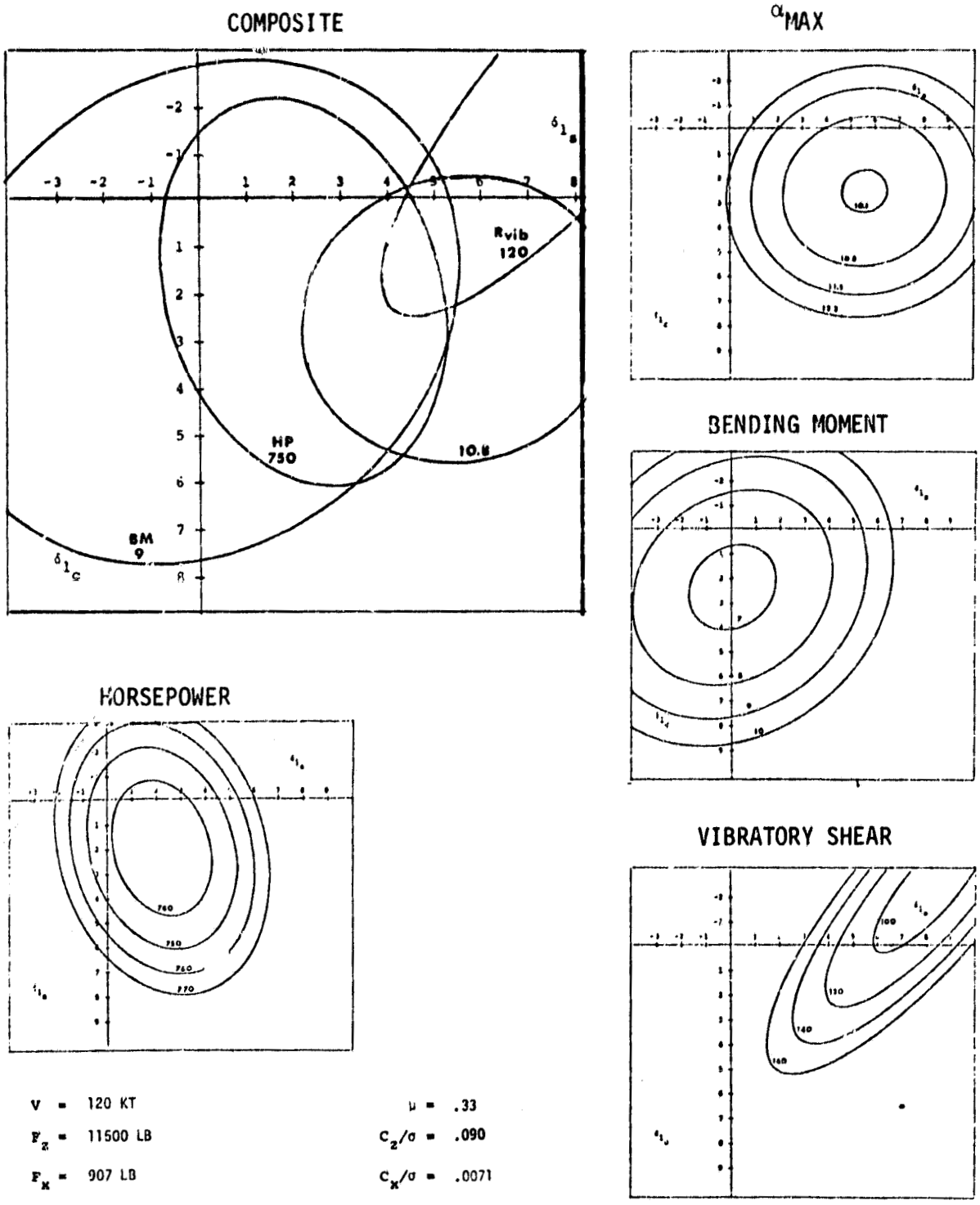

Figure 12. CTR Control Optimization; δ_0 = -4°.

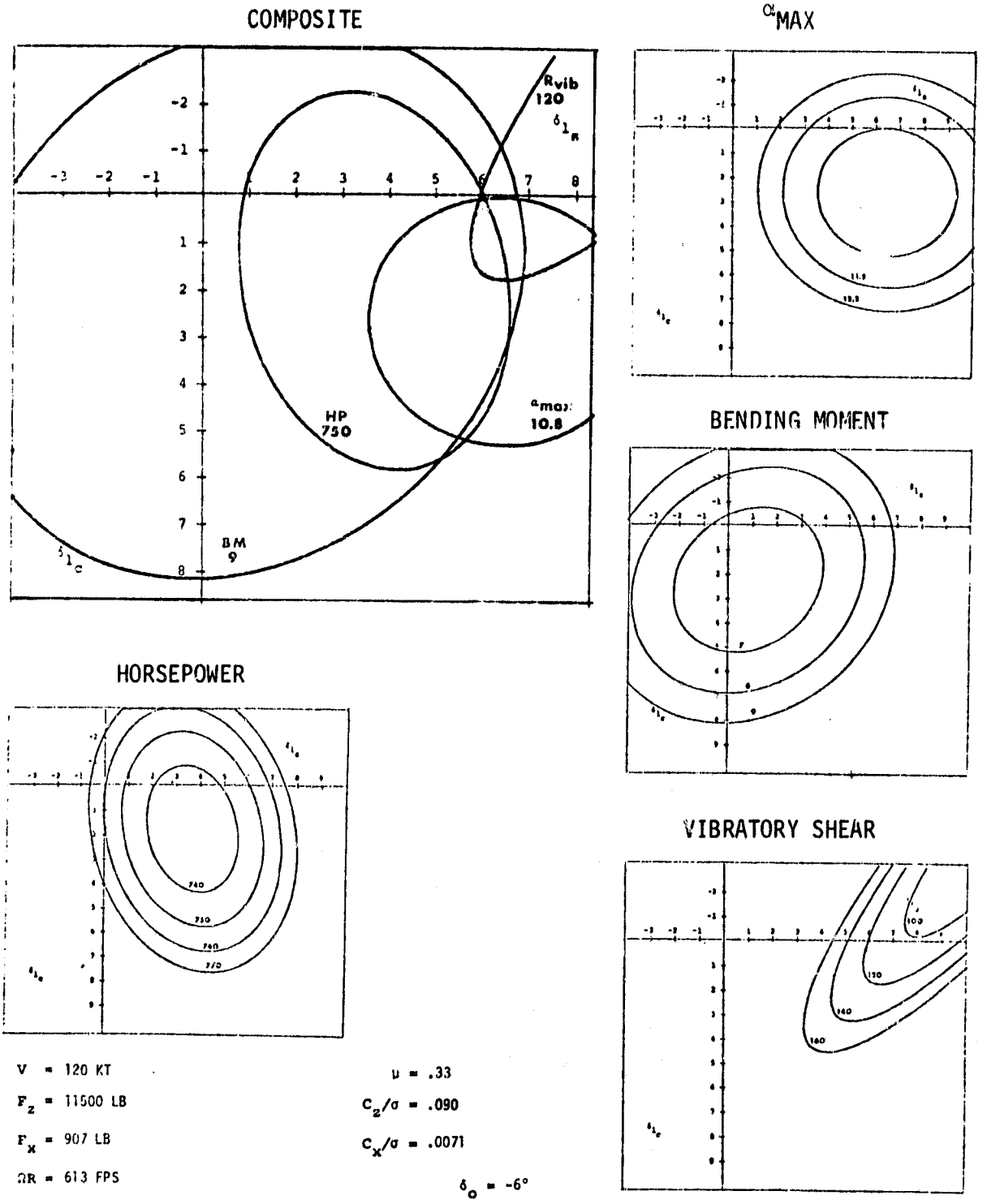

Figure 13. CTR Control Optimization, δ_0 = -6°.

For the multicyclic flap concept the range of cyclic control was limited to ±2 degrees for each harmonic component with the initial range of collective flap input being 0 to -4 degrees. The flap ranges were selected based on the CTR work that was being conducted concurrently. The cyclic inputs were restricted to limit the maximum resultant flap deflection, based on the stacking or combining of the various harmonics, to 8 degrees. Excessive flap deflection might negate the benefits of higher harmonics. The following control range was arbitrarily established as a base:

Steady: 0, -2°, -4°, -6°

First Harmonic Sine and Cosine: +2°, 0°, -2°

Second Harmonic Sine and Cosine: +2°, 0°, -2°

Third Harmonic Sine and Cosine: +2°, 0°, -2°

The selection of a control matrix by a method similar to that for the CTR was considered impractical because of the large number of control combinations possible. Restricting the problem to inputs listed above results in 2196 possible combinations. (Three control levels for each of seven controls.) A base of sixty cases was selected by use of a random number table. This method would avoid individual prejudices and statistically provides equal weight to the independent variables. Thus, the maximum chance is provided of accounting for the effects of each variable within the limited number of cases that were run.

The initial inputs of pitch horn controls, to the trim program, for each of the selected cases were based on predictions from a preliminary CTR model.

For multicyclic, a linear regression model of each independent control variable (pitch horn controls) was also modeled for each dependent variable. Due to the inclusion of the additional harmonic terms, each equation is expanded to 36 linear coefficients rather than the eleven previously required for the CTR. Equation (2) is the form of the equation with horsepower being the dependent variable used to illustrate the relationships.

$$HP = a_0 + a_1\delta_0 + a_2\delta_{1s} + a_3\delta_{1c} + a_4\delta_{2s} + a_5\delta_{2c} + a_6\delta_{3s} + a_7\delta_{3c}$$
$$+ a_8\delta_0^2 + a_9\delta_0\delta_{1s} + a_{10}\delta_0\delta_{1c} + a_{11}\delta_0\delta_{2s} + a_{12}\delta_0\delta_{2c} + a_{13}\delta_0\delta_{3s}$$
$$+ a_{14}\delta_0\delta_{3c} + a_{15}\delta_{1s}^2 + a_{16}\delta_{1s}\delta_{1c} + a_{17}\delta_{1s}\delta_{2s} + a_{18}\delta_{1s}\delta_{2c}$$
$$+ a_{19}\delta_{1s}\delta_{3s} + a_{20}\delta_{1s}\delta_{3c} + a_{21}\delta_{1c}^2 + a_{22}\delta_{1c}\delta_{2s} + a_{23}\delta_{1c}\delta_{2c}$$
$$+ a_{24}\delta_{1c}\delta_{3s} + a_{25}\delta_{1c}\delta_{3c} + a_{26}\delta_{2s}^2 + a_{27}\delta_{2s}\delta_{2c} + a_{28}\delta_{2s}\delta_{3s}$$
$$+ a_{29}\delta_{2s}\delta_{3c} + a_{30}\delta_{2c}^2 + a_{31}\delta_{2c}\delta_{3s} + a_{32}\delta_{2c}\delta_{3c} + a_{33}\delta_{3s}^2$$
$$+ a_{34}\delta_{3s}\delta_{3c} + a_{35}\delta_{3c}^2 \qquad (2)$$

where:

$$\delta = \delta_0 + \delta_{1s}\sin\psi + \delta_{1c}\cos\psi + \delta_{2s}\sin 2\psi + \delta_{2c}\cos 2\psi$$
$$+ \delta_{3s}\sin 3\psi + \delta_{3c}\cos 3\psi \qquad (3)$$

Graphical methods, previously used for prediction of optimum operating areas with 1/rev control inputs, are not possible to use with higher harmonics. For the higher harmonic control optimization, emphasis was placed on the use of the model to predict trends.

When a model was updated, a BASIC language program, MODEL 4, Appendix D, was used to test all possible flap combinations being considered to determine which combinations would meet pre-established criteria. These flap combinations were listed with the model's predictions for use in selection of future cases.

DISCUSSION OF RESULTS

CTR

Three disk loadings were examined during the CTR work preceding the multicyclic study:

$C_z/\sigma = .090$	11500 lb rotor lift
$C_z/\sigma = .098$	12500 lb rotor lift
$C_z/\sigma = .106$	13500 lb rotor lift

A total of 97 cases were trimmed during this phase of the investigation. Thirty-three of these cases were at a C_z/σ of .090; 24 of the total representing the basic flap control matrix selected to span the anticipated range of flap controls (Figure 8). The remaining cases were used to test and refine the regression models developed.

For the baseline study at 11500 lb of rotor lift, the following boundary limits were selected:

1. Horsepower $\leq$ 750
2. Four/rev pylon excitation $\leq \pm$120 lb
3. Maximum local blade angle of attack $\leq$ 10.8 deg
4. Maximum out-of-plane bending moment $\leq$ 9 in-kips
5. No. iterations to convergence η_c = 10

The angle of attack limit was chosen to provide a margin of maneuverability before local blade stall would be encountered. The 9000 in-lb peak-to-peak bending moment was selected on the basis of the calculated infinite blade life. The maximum out-of-plane moment occurs in the flap region of the blade where the endurance limit is $\pm$4500 in-lb.

After the original control matrix cases were trimmed by the aeroelastic trim program, the regression analysis program, SURGEN, was used to generate the coefficients of the five preliminary models.

On the basis of this early model, three cases, one at each collective setting, were selected to test the validity of the model. Good correlation on horsepower and η_c, fair correlation on angle of attack and bending moment and poor correlation on pylon excitation were obtained (Table 1). Examination of predicted performance contours (Figure 12) shows only one data point (P4) on the minimum vibration side of the predicted optimization area and that was too far away to define the operating area vibratory level unambiguously. Five more data points were added to the matrix to delimit the $\delta_o = -2°$ and $\delta_o = -4°$ operating area. These eight cases were added to the data file, a new model constructed and predictions obtained to validate this version of the models. The updated models predictions provided much better correlation but the pylon excitation results were still optimistic (Revised Model column of Table 1), the total of 33 trimmed cases only two have four/rev pylon loads less than the ±120 lb suggested by the model of this parameter. From a review of the actual data, Table 2, it appears that ±150 lb would be a more realistic load level to use for pylon excitation boundary. It can be seen that at each collective setting, the minimum pylon loading occurs with zero first harmonic cosine coupled with the maximum sine input (cases K3, P4, R1). However, the accompanying bending moments and horsepower of these cases exceed the boundary value selected for these parameters. In Figure 8 the four/rev pylon excitation, horsepower, local blade angle of attack, and bending moment are shown for the range of flap controls investigated. At every collective level the pylon loading is reduced by a more negative first harmonic cosine term combined with a positive sine component. Accompanying the reduction in pylon vibratory loading is an increase in horsepower and out-of-plane bending moment.

For the two remaining disk loadings the method of selection of the control matrix was altered. A reduced number of cases was used as a nucleus for a limited control model.

$$Y = a_o + a_1\delta_o + a_2\delta_{1s} + a_3\delta_{1c} + a_4\delta_o\delta_{1s} + a_5\delta_{1s}\delta_{1c} \qquad (4)$$

The resulting models were used to predict performance and trim control settings for a wide array of flap settings. Examination of these prediction tables showed the most promising direction to be toward larger positive values of δ_{1s} and δ_{1c} in conjunction with increased negative collective control. Accordingly, additional cases were selected in this direction at each of the disk loadings to fill the basic control matrices (Figures 9 and 10).

As in the case of the lower disk loadings preliminary models of the form of Equation (2) were obtained in all the dependent variables. To construct plots defining the optimum cyclic flap settings at each flap collective setting revised, boundary values were needed. By constructing a series of these contour plots for various load combinations of the

TABLE 1. CTR CONTROL OPTIMIZATION MODEL PREDICTIONS VS ACTUAL TRIM DATA

F_z = 11500 lb
F_x = 907 lb
V = 120 kt

C_z/σ = .090
ΩR = 613 fps

Rotor Parameter	Case Z1			Case Z2			Case Z3		
	Actual Trim Value	Initial Model	Revised Model	Actual Trim Value	Initial Model	Revised Model	Actual Trim Value	Initial Model	Revised Model
Four/Rev Pylon Excitation - +/- lb	172	118	144	150	118	142	156	123	139
Rotor HP	752	739	746	746	742	743	749	741	744
Max. Local Blade Angle of Attack - deg	9.7	10.3	10.1	10.1	10.4	10.1	10.4	10.5	10.4
Out Plane Bending Moment - In.-Kips D/P	8.4	7.9	8.2	8.2	8.0	8.1	8.2	7.9	8.0
Pitch Horn Collective, A_0 - deg	15.38	13.79	15.26	13.96	15.18	13.86	12.61	12.45	12.49
Pitch Horn - First Harmonic Input B1S - deg	4.60	3.90	4.39	4.3	4.2	4.09	4.00	3.65	3.78
Pitch Horn - First Harmonic Input A1S - deg	-2.13	-1.54	-2.07	-1.58	-2.03	-1.60	-1.11	-1.10	-1.14

TABLE 2. MFS CONTROL STUDY, SUMMARY OF CTR CONTROL OPTIMIZATION

F_z = 11500 lb F_x = 907 lb

CASE NO	FLAP DO	INPUT-DEG D1S	D1C	FOUR/REV PYLON LOADING KIPS	ROTOR HP	MAX LOCAL BLADE ANGLE OF ATTACK DEG	BENDING MOMENT OP IN-KIPS P/P	PITCH HORN INPUT DEGREES A0	B1S	A1S
K1	0.0	0.0	0.0	172.	747.	12.0	8.3	16.62	6.19	0.05
K2	0.0	0.0	4.0	197.	755.	10.9	8.6	16.59	5.69	-4.50
K3	0.0	4.0	0.0	97.	813.	11.3	10.4	17.73	1.88	0.71
K6	0.0	-4.0	0.0	389.	767.	15.6	9.0	16.50	10.70	-0.50
K5	0.0	-4.0	4.0	255.	766.	13.8	8.2	16.27	10.00	-5.00
K7	0.0	0.0	8.0	277.	779.	13.1	10.4	16.50	5.00	-8.86
K8	0.0	-4.0	8.0	202.	798.	15.7	9.6	16.30	9.55	-9.52
O0	-4.0	0.0	0.0	250.	744.	12.6	7.0	13.61	8.56	-0.52
P5	-4.0	0.0	4.0	226.	750.	12.4	7.2	13.55	8.15	-4.89
O4	-4.0	-4.0	0.0	780.	818.	17.6	9.4	14.16	13.64	-1.24
O5	-4.0	4.0	0.0	142.	744.	10.7	8.3	13.90	4.30	-0.02
O6	-4.0	-4.0	4.0	379.	818.	15.9	7.6	13.77	12.90	-5.70
O7	-4.0	4.0	4.0	150.	751.	10.5	8.5	13.84	3.80	-4.36
P1	-4.0	-4.0	8.0	314.	897.	18.9	10.2	14.70	13.80	-10.60
P2	-4.0	0.0	8.0	252.	776.	14.2	9.2	13.40	7.50	-9.50
P3	-4.0	4.0	8.0	241.	774.	12.6	11.0	13.77	3.10	-8.83
O2	-8.0	0.0	0.0	525.	786.	14.4	6.4	11.10	11.30	-1.33
O3	-8.0	0.0	4.0	346.	796.	14.2	6.3	10.80	10.70	-5.77
O8	-8.0	4.0	0.0	247.	754.	12.3	6.5	11.00	6.60	-0.57
O9	-8.0	4.0	4.0	209.	755.	12.0	6.6	10.00	10.73	-4.89
R1	-8.0	8.0	0.0	144.	758.	11.2	9.1	11.30	2.58	-0.02
R2	-8.0	8.0	4.0	162.	765.	10.8	9.5	11.20	1.92	-4.40
R3	-8.0	4.0	8.0	293.	790.	13.4	9.8	10.90	5.80	-9.20
R4	-8.0	0.0	8.0	273.	844.	15.9	9.3	11.37	10.91	-10.13
P4	-4.0	8.0	0.0	111.	800.	10.6	11.4	14.80	0.0	0.64
P6	-4.0	6.0	2.0	140.	766.	9.2	9.8	14.25	1.96	-1.86
Z1	-2.0	2.5	2.0	172.	752.	9.7	8.4	15.38	4.60	-2.13
Z2	-4.0	4.0	1.5	150.	746.	10.1	8.2	13.96	4.30	-1.58
Z3	-6.0	5.5	1.0	156.	749.	10.6	8.2	12.61	4.00	-1.11
S1	-2.0	2.0	0.0	170.	747.	10.6	8.3	15.39	5.50	0.01
S2	-2.0	4.0	0.0	159.	766.	10.8	9.6	15.73	3.23	0.35
S3	-2.0	4.0	2.0	166.	764.	9.1	9.4	15.59	2.89	-1.91
P7	-4.0	6.0	0.0	133.	766.	10.3	9.8	14.30	2.29	0.29

performance parameters it was apparent that all the parameters did not optimize at the same flap settings. Clear optimums were noted for each parameter and the differences had to be compromised to give the best trade-off. Desirable operation was defined as simultaneously meeting these criteria:

	C_z/σ = .098	C_z/σ = .106
Horsepower	$\leq$ 790	$\leq$ 820
Max. Local Blade Angle of Attack	$\leq$ 11.5 deg	$\leq$ 12.5 deg
Max. Out-of-Plane Bending Moment	$\leq$ 9 in -kips	$\leq$ 9 in -kips
Pylon Excitation	$\leq$ 180 lb	$\leq$ 260 lb
No. of Iterations to Converge	$\leq$ 10	$\leq$ 10

With these criteria the contour plots indicate that at C_z/σ of .098, a small area of acceptable operation exists at $\delta_0 = 0°$. This area grows larger at more negative collective setting, then at $\delta_0 = -6°$ no desirable area exists. Defining optimum as the collective with the largest desirable operating range the parameters may be traded off to some extent for further improvement. A correlation case based on the preliminary model produced good correlation except for the optimistic pylon excitation. Three additional cases were set up to weigh the model in the vicinity of optimum. These cases were trimmed, added to the data base (total 31 cases;) and used to refine the model. Table 3 indicates the results of the predicted and actual data obtained. As was the case at the lower disk loading, correlation is excellent with the exception of the four/rev pylon excitation which is optimistic for all cases.

A review of the actual pylon forces (Table 4) indicates that all the trimmed cases but Z7 exceed the ±180 lb criterion established for our modeled plot program boundary. The general trend toward a reduced pylon excitation force moving toward the lower positive δ_{1s} and to zero δ_{1c} that was obtained for the lower C_z/σ was maintained at this level (Figure 9). The results of the four cases in the predicted optimum area ($\delta_0 = -2.5$ deg) would indicate that this region would give the minimum pylon loading of ±200 lb and maintain acceptable values of the other rotor parameters. Collective levels of -3 deg and -5 deg do produce lower pylon loads but a penalty of higher bending moments and horsepower is imposed.

TABLE 3. MFS CONTROL STUDY MODEL PREDICTION VS ACTUAL TRIM DATA

F_z = 12500 lb
F_x = 907 lb
V = 120 kt

C_z/σ = .098
ΩR = 613 fps

Rotor Parameter	Case Z1		Case Z7		Case Z8		Case Z9	
	Actual Trim Value	Model	Actual Trim Value	Model	Actual Trim Value	Model	Actual Trim Value	Model
Four/Rev Pylon Excitation - +/- lb	197	168	174	172	196	174	198	169
Rotor HP	786	783	769	781	785	782	787	783
Max. Local Blade Angle of Attack - deg	11.0	10.9	10.8	11.0	11.2	11.1	10.8	10.8
Out-of-Plane Bending Moment - In -Kips P/P	9.1	8.9	8.6	8.5	8.8	8.6	9.0	8.8
Pitch Horn Collective - A_0 - deg	15.95	15.82	15.75	15.74	15.90	15.79	15.92	15.78
Pitch Horn - First Harmonic Input B1S - deg	4.34	4.35	4.29	4.69	4.79	4.74	4.27	4.30
Pitch Horn - First Harmonic Input A1S - deg	-1.72	-1.86	-2.42	-2.43	-1.78	-1.86	-2.23	-2.45

TABLE 4. MFS CONTROL STUDY, SUMMARY OF CTR OPTIMIZATION

F_z = 12500 lb F_x = 907 lb

CASE NO	FLAP INPUTS -DEGREES									PYLON EXCITATION +/- LBS	HORSEPOWER	OP BENDING MOMENT +/- IN-LBS	MAX LOCAL ANGLE OF ATTACK-DEG	PITCH HORN INPUT DEGREES		
	D0	D1S	D1C	D2S	D2C	D3S	D3C	D4S	D4C					A0	B1S	A1S
F1	-3.0	2.0	3.0	0.0	0.0	0.0	0.0	0.0	0.0	215.	787.	8.	11.7	15.30	5.70	-3.30
F2	-3.0	2.0	0.0	0.0	0.0	0.0	0.0	0.0	0.0	232.	787.	8.	12.8	15.50	6.10	-0.20
F3	-3.0	-1.0	0.0	0.0	0.0	0.0	0.0	0.0	0.0	539.	817.	9.	15.3	15.60	9.50	-0.70
F4	-3.0	-1.0	3.0	0.0	0.0	0.0	0.0	0.0	0.0	370.	814.	8.	13.7	15.32	8.98	-3.89
F5	-3.0	2.0	6.0	0.0	0.0	0.0	0.0	0.0	0.0	237.	799.	8.	12.8	15.10	5.30	-5.50
F6	-3.0	5.0	3.0	0.0	0.0	0.0	0.0	0.0	0.0	184.	795.	10.	10.5	15.50	3.90	-2.90
F7	-3.0	-1.0	6.0	0.0	0.0	0.0	0.0	0.0	0.0	264.	826.	8.	14.9	15.17	8.62	-7.17
Z4	0.0	1.5	3.0	0.0	0.0	0.0	0.0	0.0	0.0	216.	786.	9.	10.9	17.53	4.89	-2.98
Z5	3.0	-2.0	0.0	0.0	0.0	0.0	0.0	0.0	0.0	280.	807.	10.	14.8	19.90	7.36	0.03
G1	-5.0	2.0	3.0	0.0	0.0	0.0	0.0	0.0	0.0	278.	794.	7.	12.9	13.94	6.84	-3.74
G2	-5.0	2.0	0.0	0.0	0.0	0.0	0.0	0.0	0.0	332.	790.	8.	13.3	14.15	7.30	-0.53
G3	-5.0	-1.0	0.0	0.0	0.0	0.0	0.0	0.0	0.0	902.	866.	11.	17.3	15.00	11.65	-1.10
G4	-5.0	-1.0	3.0	0.0	0.0	0.0	0.0	0.0	0.0	494.	848.	8.	15.1	14.30	10.70	-4.40
G5	-5.0	2.0	6.0	0.0	0.0	0.0	0.0	0.0	0.0	262.	815.	8.	13.6	13.80	6.50	-7.00
G6	-5.0	5.0	3.0	0.0	0.0	0.0	0.0	0.0	0.0	192.	788.	9.	11.3	14.00	3.70	-3.20
G7	-5.0	-1.0	6.0	0.0	0.0	0.0	0.0	0.0	0.0	347.	877.	8.	16.3	14.40	10.65	-7.80
Z6	-7.0	8.0	0.0	0.0	0.0	0.0	0.0	0.0	0.0	197.	802.	10.	12.0	13.11	2.38	-0.04
Z1	-7.0	2.0	3.0	0.0	0.0	0.0	0.0	0.0	0.0	381.	824.	7.	13.9	12.75	8.31	-4.26
Z3	-5.0	5.5	1.0	0.0	0.0	0.0	0.0	0.0	0.0	193.	792.	9.	11.4	14.35	3.72	-1.07
X5	-7.0	2.0	6.0	0.0	0.0	0.0	0.0	0.0	0.0	325.	843.	8.	14.6	12.73	8.10	-7.55
Z2	-1.0	1.0	3.5	0.0	0.0	0.0	0.0	0.0	0.0	218.	784.	8.	11.6	16.72	5.72	-3.72
X1	-1.0	2.0	3.0	0.0	0.0	0.0	0.0	0.0	0.0	211.	795.	9.	10.9	16.80	4.80	-3.10
X2	-1.0	2.0	0.0	0.0	0.0	0.0	0.0	0.0	0.0	222.	792.	9.	12.6	16.94	5.15	0.05
X4	-1.0	-1.0	3.0	0.0	0.0	0.0	0.0	0.0	0.0	258.	789.	8.	12.6	16.52	7.60	-3.50
X5	-1.0	2.0	6.0	0.0	0.0	0.0	0.0	0.0	0.0	240.	792.	9.	12.2	16.50	4.34	-6.10
X6	-1.0	5.0	3.0	0.0	0.0	0.0	0.0	0.0	0.0	208.	794.	11.	9.8	16.90	2.05	-2.70
X7	-1.0	-1.0	6.0	0.0	0.0	0.0	0.0	0.0	0.0	257.	799.	9.	13.8	16.37	7.25	-6.64
Z7	-2.5	3.0	2.2	0.0	0.0	0.0	0.0	0.0	0.0	174.	769.	9.	10.8	15.75	4.26	-2.42
Z1	-2.5	3.5	1.7	0.0	0.0	0.0	0.0	0.0	0.0	197.	786.	9.	11.0	15.95	4.34	-1.72
Z8	-2.5	3.0	1.7	0.0	0.0	0.0	0.0	0.0	0.0	196.	785.	9.	11.2	15.90	4.79	-1.78
Z9	-2.5	3.5	2.2	0.0	0.0	0.0	0.0	0.0	0.0	198.	787.	9.	10.8	15.92	4.27	-2.23

The final CTR disk loading of C_z/σ of .106 was developed concurrently with the 12500 lb rotor loading and followed the same philosophy on optimization (Table 5). Restrictive models (Equation 4) were used to predict the optimum direction of flap controls. The control matrix was filled, cases trimmed, contour plots constructed and an area of desirable operation defined. For the predicted region of optimization, additional cases were selected and trimmed to correlate and update the models. Referring to Figure 10, δ_0 = -4 deg appears to be the best collective level to operate. Lower pylon loads can be obtained at δ_0 = -3 deg but the horsepower and bending moments become excessive. A pylon excitation of ±250 lb appears to be a realistic limit at this disk loading. This is reinforced by the good correlation obtained for all the parameters (Table 6).

It has been observed that the number of iterations to converge depends on the flap control input being trimmed to a particular flight condition. At 12500 lb rotor lift, the number of iterations to converge was explored for 22 trim cases over a wide range of collective and cyclic flap settings.

Using the mathematical model developed by SURGEN contours for η_c = 6, 8, 10 and 12 were plotted for collective settings of 0°, -1°, and -3°. It was found that optimum performance areas uniformly lay within η_c < 10 contours. If η_c is a measure of stability, it seems that stability should not constrain performance operation. Therefore, this parameter was not considered for the multicyclic study.

Multicyclic Flap Inputs

The multicyclic investigation was performed at C_z/σ = .090, μ = .333 (120 knots) since 134 of the 157 trimmed cases were at this rotor loading (11500 lb). This disk loading allows direct comparison with the CTR evaluated at this level.

The collective range of 0° to -4° of the original sixty randomly selected cases was extended to include both the -6° and -8° region when early trends indicated promising results with more negative collective. The -8° level was discontinued when the four/rev pylon excitation loads derived at this collective setting proved extremely high.

TABLE 5. MFS CONTROL STUDY MODEL PREDICTIONS VS ACTUAL TRIM DATA

F_z = 13500 lb
F_x = 907 lb
V = 120 kt

C_z/σ = .106
ΩR = 613 fps

	Case P1			Case P2			Case P3			Case P4		
Rotor Parameter	Actual Trim Value	Initial Model	Revised Model	Actual Trim Value	Initial Model	Revised Model	Actual Trim Value	Initial Model	Revised Model	Actual Trim Value	Initial Model	Revised Model
Four/Rev Pylon Excitation - +/- lb	252	203	231	242	188	218	234	177	205	238	192	219
Rotor HP	820	809	815	818	806	812	816	805	812	819	808	814
Max. Local Blade Angle of Attack - deg	12.5	11.9	12.2	12.1	11.5	11.9	11.8	11.3	11.7	12.2	11.5	11.9
Out-of-Plane Bending Moment - In.-Kips P/P	9.3	8.9	9.1	9.5	9.1	9.4	9.9	9.4	9.6	10.0	9.5	9.7
Pitch Horn Collective - A0 - deg	15.70	15.35	15.57	15.73	15.39	15.61	15.78	15.45	15.67	15.74	15.38	15.61
Pitch Horn - First Harmonic Input B1S - deg	4.00	3.69	3.88	3.56	3.24	3.42	3.14	2.82	3.01	3.03	2.70	-2.90
Pitch Horn - First Harmonic Input A1S - deg	-4.12	-4.11	-4.11	-3.50	-3.48	-3.49	-2.90	-2.87	-2.88	-3.95	-3.94	-3.94

TABLE 6. MFS CONTROL STUDY, SUMMARY OF CTR CONTROL OPTIMIZATION

F_z = 13500 lb F_x = 907 lb

CASE NO	FLAP INPUTS -DEGREES									PYLON EXCITATION +/- LBS	HORSEPOWER	OP BENDING MOMENT +/- IN-LBS	MAX LOCAL ANGLE OF ATTACK-DEG	PITCH HORN INPUT DEGREES		
	D0	D1S	D1C	D2S	D2C	D3S	D3C	D4S	D4C					A0	B1S	A1S
J1	-3.0	2.0	6.0	0.0	0.0	0.0	0.0	0.0	0.0	288.	840.	9.	14.3	16.10	5.70	-6.70
J3	-3.0	5.0	0.0	0.0	0.0	0.0	0.0	0.0	0.0	232.	824.	11.	13.3	16.75	3.60	0.12
J5	-3.0	8.0	0.0	0.0	0.0	0.0	0.0	0.0	0.0	138.	848.	12.	12.7	17.08	0.92	3.44
C5	-3.0	2.0	3.0	0.0	0.0	0.0	0.0	0.0	0.0	317.	823.	9.	13.2	16.37	6.20	-3.50
C6	-3.0	2.0	0.0	0.0	0.0	0.0	0.0	0.0	0.0	494.	838.	11.	15.2	16.92	6.94	-0.28
C7	-3.0	5.0	3.0	0.0	0.0	0.0	0.0	0.0	0.0	224.	817.	10.	11.6	16.30	2.90	-3.00
C8	-3.0	5.0	6.0	0.0	0.0	0.0	0.0	0.0	0.0	252.	818.	10.	13.0	16.20	2.70	-6.20
J6	-3.0	8.0	3.0	0.0	0.0	0.0	0.0	0.0	0.0	232.	826.	12.	11.1	16.68	0.42	-2.62
H1	-5.0	2.0	3.0	0.0	0.0	0.0	0.0	0.0	0.0	428.	859.	8.	14.2	15.10	7.50	-4.00
H2	-5.0	2.0	0.0	0.0	0.0	0.0	0.0	0.0	0.0	755.	878.	11.	16.1	16.05	8.78	-0.40
H3	-5.0	5.0	0.0	0.0	0.0	0.0	0.0	0.0	0.0	192.	931.	11.	12.6	15.50	1.70	0.22
H5	-5.0	5.0	3.0	0.0	0.0	0.0	0.0	0.0	0.0	252.	821.	9.	12.5	14.90	3.90	-3.30
H6	-5.0	5.0	6.0	0.0	0.0	0.0	0.0	0.0	0.0	288.	841.	10.	13.6	14.80	3.70	-6.60
H7	-5.0	2.0	6.0	0.0	0.0	0.0	0.0	0.0	0.0	363.	872.	9.	15.5	15.26	7.44	-7.40
N1	-5.0	5.0	0.0	0.0	0.0	0.0	0.0	0.0	0.0	308.	828.	10.	13.4	15.40	4.70	-0.70
N2	-5.0	8.0	3.0	0.0	0.0	0.0	0.0	0.0	0.0	210.	824.	11.	11.5	15.20	1.27	-2.90
L1	-1.0	-1.0	3.0	0.0	0.0	0.0	0.0	0.0	0.0	470.	850.	10.	14.9	17.85	8.40	-3.65
L3	-1.0	2.0	3.0	0.0	0.0	0.0	0.0	0.0	0.0	256.	819.	9.	12.0	17.57	4.84	-3.12
L2	-1.0	-1.0	6.0	0.0	0.0	0.0	0.0	0.0	0.0	300.	864.	9.	15.9	17.70	8.00	-6.90
L4	-1.0	2.0	6.0	0.0	0.0	0.0	0.0	0.0	0.0	274.	824.	9.	13.7	17.40	4.50	-6.20
L5	-1.0	5.0	3.0	0.0	0.0	0.0	0.0	0.0	0.0	220.	820.	11.	11.0	17.76	2.10	-2.74
L6	-1.0	2.0	0.0	0.0	0.0	0.0	0.0	0.0	0.0	318.	834.	11.	14.7	18.14	5.58	0.02
L7	-1.0	5.0	0.0	0.0	0.0	0.0	0.0	0.0	0.0	185.	844.	11.	13.6	18.37	2.78	0.36
L0	-1.0	-1.0	0.0	0.0	0.0	0.0	0.0	0.0	0.0	1073.	929.	14.	19.1	19.40	10.30	-0.48
L9	-1.0	5.0	6.0	0.0	0.0	0.0	0.0	0.0	0.0	286.	821.	11.	12.6	17.70	1.90	-5.86
Y1	-3.0	3.5	3.0	0.0	0.0	0.0	0.0	0.0	0.0	260.	815.	9.	12.4	16.28	4.56	-3.25
Y2	-4.0	4.5	2.8	0.0	0.0	0.0	0.0	0.0	0.0	256.	818.	9.	12.3	15.76	4.13	-3.06
Y3	-5.0	5.5	3.0	0.0	0.0	0.0	0.0	0.0	0.0	244.	822.	9.	12.2	15.11	3.64	-3.30
P1	-4.0	4.5	3.8	0.0	0.0	0.0	0.0	0.0	0.0	252.	820.	9.	12.5	15.70	4.00	-4.12
P2	-4.0	5.0	3.3	0.0	0.0	0.0	0.0	0.0	0.0	242.	818.	10.	12.1	15.78	3.56	-3.50
P3	-4.0	5.5	2.8	0.0	0.0	0.0	0.0	0.0	0.0	234.	816.	10.	11.8	15.78	3.14	-2.90
P4	-4.0	5.5	3.8	0.0	0.0	0.0	0.0	0.0	0.0	238.	819.	10.	12.2	15.74	3.03	-3.95

Due to the complexity of the system as a result of the addition of the second and third flap harmonics, heavy emphasis was placed on the predictions of the models in selection of future cases. As was the case with the CTR segment of this study, the shear predictions of early models were extremely optimistic. However, the trends indicated by these models were correct. A review of the case listings (Table 7) showed a general reduction of pylon loads after the first sixty cases. This was attributed to the weighting of the model toward lower pylon loads by the exclusion from the model of cases with extreme values of this parameter as additional cases become available.

At the 11500 lb load level with first harmonic flap input (CTR), ±150 lb of pylon excitation appears to be the minimum value obtainable when tradeoffs with the other rotor parameters are made. Listed in Table 8 are the 18 trimmed cases with four/rev pylon loads less than ±150 lb. The majority of these cases are at a collective setting of -4° which corresponds to the most desirable collective for the CTR at this load level. Restricting ourselves to the -4° level it should be noted that the six cases with the lowest pylon excitation loads have no third harmonic flap input. The two remaining cases have only the sine component of third harmonic. Referring to Table 9, holding the collective and first harmonic sine constant at $\delta_0 = -4°$ and $\delta_{1s} = -2°$, respectively, (no third harmonic) the pylon excitation is reduced with more positive first harmonic cosine input (cases Z5, Z7, B9, N7). As was the case with the CTR baseline rotor, a reduction in pylon force was accompanied by adverse effects on the other rotor parameters. A drawback to the MFS appears to be its effect on local blade angle of attack. In general, MFS induces higher local angles of attack than exhibited by the CTR. The remaining criteria, horsepower, and blade bending moment are within the acceptable limits established. By inspection of Table 9 the optimum operating point corresponds to trim point Z7. The ±94 lb of pylon excitation is 40 percent lower than the minimum value at the CTR optimum trim point 05 (±142 lb). Operation at this speed and gross weight with a fixed second harmonic input ($\delta_{2s} = 2°$; $\delta_{2c} = -2°$) and no third harmonic will produce acceptable results with zero or negative first harmonic input. The pylon loading in this control range will be substantially below that obtained for the CTR.

Table 10 is a comparison of the pitch horn controls, horsepower and bending moments obtained by the trim program and the values predicted by our updated model. The correlation obtained is good considering the small percentage of cases trimmed.

A point to stress in this study is that 4.7 percent of a total of 2916 possible flap combinations were trimmed to generate this data. When experience is gained in the selection of cases and use of these models, this figure can be reduced. Two other points should be noted about results of this study.

TABLE 7. MFS CONTROL STUDY, SUMMARY OF TRIMMED CASES

F_z = 11500 lb
F_x = 907 lb

C_z/σ = .090
ΩR = 613 fps

CASE NO	FLAP INPUTS -DEGREES									PYLON EXCITATION +/- LBS	HORSEPOWER	OP BENDING MOMENT +/- IN-LBS	MAX LOCAL ANGLE OF ATTACK-DEG	PITCH HORN INPUT DEGREES		
	D0	D1S	D1C	D2S	D2C	D3S	D3C	D4S	D4C					A0	B1S	A1S
A0	0.0	-2.0	-2.0	2.0	-2.0	2.0	0.0	0.0	0.0	493.	747.	4600.	12.8	16.31	7.48	1.04
A1	-2.0	-2.0	0.0	2.0	-2.0	-2.0	-2.0	0.0	0.0	436.	777.	3800.	13.7	14.62	8.43	-1.61
A2	-2.0	2.0	2.0	-2.0	-2.0	2.0	2.0	0.0	0.0	610.	777.	6850.	13.8	15.23	4.10	-0.67
A3	-2.0	0.0	0.0	-2.0	-2.0	0.0	0.0	0.0	0.0	183.	746.	4770.	13.4	14.88	6.57	0.93
A4	0.0	0.0	-2.0	-2.0	0.0	0.0	2.0	0.0	0.0	771.	856.	9000.	18.3	17.88	7.00	3.62
A5	0.0	-2.0	2.0	2.0	2.0	2.0	-2.0	0.0	0.0	606.	915.	5940.	21.8	19.20	12.10	-4.38
A6	-2.0	0.0	-2.0	2.0	0.0	0.0	2.0	0.0	0.0	331.	752.	4015.	12.8	15.27	7.63	0.79
A7	-2.0	2.0	2.0	2.0	2.0	0.0	0.0	0.0	0.0	418.	771.	4645.	14.0	15.87	6.14	-3.62
A8	0.0	0.0	2.0	0.0	-2.0	0.0	-2.0	0.0	0.0	485.	774.	4220.	8.6	16.42	4.95	-2.05
A9	0.0	0.0	2.0	0.0	-2.0	-2.0	0.0	0.0	0.0	382.	789.	4910.	10.0	16.40	4.95	-2.03
B0	-4.0	2.0	-2.0	2.0	2.0	-2.0	0.0	0.0	0.0	395.	799.	3540.	16.6	15.32	9.39	0.46
B1	-4.0	2.0	-2.0	-2.0	2.0	2.0	0.0	0.0	0.0	1935.	918.	11330.	23.7	17.10	10.60	3.60
B2	-2.0	-2.0	0.0	0.0	2.0	2.0	0.0	0.0	0.0	1581.	864.	8590.	21.6	17.00	12.19	-0.60
B3	-4.0	2.0	0.0	2.0	0.0	0.0	-2.0	0.0	0.0	458.	758.	3985.	12.6	13.83	6.32	-1.40
B4	-4.0	-2.0	2.0	0.0	-2.0	-2.0	2.0	0.0	0.0	383.	767.	4090.	13.0	12.99	9.37	-3.08
B5	-4.0	2.0	2.0	-2.0	2.0	2.0	-2.0	0.0	0.0	1074.	807.	7700.	19.1	15.36	8.79	-1.10
B6	-2.0	2.0	-2.0	-2.0	0.0	2.0	2.0	0.0	0.0	1133.	845.	10120.	19.1	16.75	6.23	3.83
B7	-2.0	-2.0	-2.0	0.0	-2.0	2.0	-2.0	0.0	0.0	637.	761.	5110.	15.2	15.00	9.00	1.85
B8	0.0	2.0	0.0	0.0	0.0	0.0	2.0	0.0	0.0	482.	777.	5820.	12.6	17.16	3.97	0.36
B9	-4.0	-2.0	2.0	2.0	-2.0	0.0	0.0	0.0	0.0	73.	764.	3220.	13.2	13.03	9.24	-4.00
C0	-4.0	2.0	0.0	0.0	2.0	0.0	2.0	0.0	0.0	595.	768.	4735.	13.8	14.52	7.97	-0.49
C1	0.0	2.0	-2.0	2.0	2.0	-2.0	2.0	0.0	0.0	383.	793.	4560.	14.1	17.80	5.75	1.23
C2	-2.0	-2.0	-2.0	-2.0	0.0	2.0	2.0	0.0	0.0	1452.	852.	10400.	21.5	16.45	10.71	3.11
C3	0.0	0.0	0.0	-2.0	0.0	2.0	-2.0	0.0	0.0	719.	780.	7550.	17.1	17.43	6.98	1.43
C4	-2.0	0.0	-2.0	-2.0	0.0	-2.0	0.0	0.0	0.0	393.	792.	5610.	15.2	15.83	8.44	2.92
C5	0.0	0.0	0.0	-2.0	2.0	-2.0	2.0	0.0	0.0	780.	814.	11510.	15.7	17.84	8.11	0.89
C6	-4.0	2.0	-2.0	2.0	2.0	-2.0	2.0	0.0	0.0	399.	791.	3620.	16.4	15.11	9.00	0.33
C7	-2.0	2.0	-2.0	2.0	2.0	0.0	0.0	0.0	0.0	498.	761.	4500.	13.9	16.07	7.00	0.93
C8	-4.0	2.0	0.0	-2.0	2.0	-2.0	2.0	0.0	0.0	719.	782.	5430.	15.3	14.70	8.37	0.46
C9	-2.0	0.0	-2.0	-2.0	-2.0	-2.0	2.0	0.0	0.0	570.	829.	8570.	16.0	15.57	6.98	3.20
D0	-2.0	2.0	0.0	2.0	-2.0	0.0	2.0	0.0	0.0	366.	766.	5980.	11.6	15.00	3.90	-0.85
D1	-2.0	-2.0	2.0	0.0	2.0	2.0	2.0	0.0	0.0	1312.	821.	6660.	17.8	16.16	11.00	-3.09
D2	-2.0	-2.0	2.0	-2.0	0.0	-2.0	2.0	0.0	0.0	519.	760.	4070.	12.9	14.94	9.53	-1.86
D3	-4.0	2.0	-2.0	-2.0	2.0	0.0	0.0	0.0	0.0	1349.	877.	9140.	21.0	16.61	10.43	3.31
D4	-2.0	-2.0	2.0	0.0	2.0	2.0	0.0	0.0	0.0	1187.	821.	7130.	19.0	16.23	11.12	-2.93
D5	-2.0	-2.0	-2.0	-2.0	-2.0	-2.0	-2.0	0.0	0.0	1420.	1081.	9590.	27.7	20.15	16.03	2.77
D6	0.0	-2.0	0.0	-2.0	-2.0	-2.0	0.0	0.0	0.0	309.	765.	4530.	13.0	16.30	7.60	0.81
D7	-4.0	2.0	0.0	-2.0	-2.0	-2.0	2.0	0.0	0.0	525.	791.	5740.	13.5	13.66	5.56	0.84
D8	-2.0	-2.0	2.0	0.0	2.0	0.0	-2.0	0.0	0.0	1271.	872.	7490.	22.2	17.13	12.59	-2.89
D9	0.0	2.0	-2.0	-2.0	2.0	-2.0	-2.0	0.0	0.0	632.	910.	5830.	17.7	19.72	7.71	4.00
E0	-2.0	0.0	-2.0	0.0	0.0	0.0	2.0	0.0	0.0	410.	764.	5661.	14.8	15.49	7.78	1.93
E1	-4.0	-2.0	-2.0	-2.0	2.0	-2.0	2.0	0.0	0.0	1960.	1103.	11130.	25.6	18.59	17.12	1.91
E2	0.0	2.0	0.0	-2.0	-2.0	-2.0	2.0	0.0	0.0	786.	872.	8440.	15.0	17.47	3.50	1.56
E3	-4.0	-2.0	-2.0	2.0	2.0	0.0	0.0	0.0	0.0	2119.	1131.	10350.	25.8	19.32	17.80	-1.20
E4	-2.0	2.0	-2.0	0.0	-2.0	2.0	0.0	0.0	0.0	560.	769.	5690.	13.7	15.38	4.56	2.53

TABLE 7 (Continued)

CASE NO	FLAP INPUTS -DEGREES									PYLON EXCITATION +/- LBS	HORSEPOWER	OP BENDING MOMENT +/- IN-LBS	MAX LOCAL ANGLE OF ATTACK-DEG	PITCH HORN INPUT DEGREES		
	D0	D1S	D1C	D2S	D2C	D3S	D3C	D4S	D4C					A0	B1S	A1S
E5	-4.0	-2.0	0.0	0.0	-2.0	-2.0	-2.0	0.0	0.0	301.	762.	2410.	12.9	13.11	9.83	-0.89
E6	0.0	2.0	2.0	0.0	2.0	0.0	-2.0	0.0	0.0	474.	766.	5663.	13.9	17.40	4.91	-2.15
E7	-2.0	2.0	0.0	-2.0	-2.0	0.0	-2.0	0.0	0.0	248.	768.	4425.	11.8	15.24	4.59	1.23
E8	-2.0	2.0	2.0	-2.0	-2.0	2.0	0.0	0.0	0.0	563.	744.	5270.	14.2	14.71	8.41	-1.43
E9	-4.0	0.0	0.0	0.0	2.0	2.0	-2.0	0.0	0.0	1644.	883.	8590.	22.5	16.22	12.11	-0.53
F0	-2.0	0.0	0.0	2.0	-2.0	-2.0	-2.0	0.0	0.0	507.	783.	4500.	12.1	14.82	6.17	-1.34
F1	-4.0	2.0	0.0	-2.0	0.0	2.0	2.0	0.0	0.0	840.	784.	7710.	16.6	14.42	6.89	1.12
F2	-2.0	2.0	0.0	2.0	0.0	0.0	-2.0	0.0	0.0	556.	763.	4470.	11.8	15.37	5.00	-1.24
F3	0.0	-2.0	0.0	-2.0	0.0	-2.0	2.0	0.0	0.0	546.	794.	6150.	15.0	16.94	8.84	0.70
F4	0.0	0.0	0.0	-2.0	-2.0	-2.0	0.0	0.0	0.0	417.	801.	5620.	13.2	16.74	5.50	1.16
F5	-2.0	0.0	2.0	0.0	2.0	2.0	-2.0	0.0	0.0	1047.	789.	7210.	17.9	16.09	8.70	-2.50
F6	-4.0	2.0	2.0	-2.0	0.0	0.0	-2.0	0.0	0.0	228.	746.	4060.	13.2	13.91	6.72	-1.34
F7	-2.0	2.0	0.0	0.0	2.0	-2.0	-2.0	0.0	0.0	350.	746.	4465.	16.0	16.32	7.49	-0.18
F8	-4.0	2.0	-2.0	2.0	0.0	0.0	-2.0	0.0	0.0	410.	758.	3740.	12.9	13.94	6.74	0.74
F9	0.0	-2.0	-2.0	2.0	-2.0	-2.0	-2.0	0.0	0.0	478.	781.	4450.	12.6	16.30	7.49	0.87
G0	-6.0	-2.0	-2.0	2.0	0.0	0.0	-2.0	0.0	0.0	1266.	892.	5790.	20.7	14.13	14.40	-0.53
G3	-6.0	0.0	0.0	-2.0	0.0	0.0	2.0	0.0	0.0	614.	783.	5330.	15.9	12.59	10.21	0.21
G5	-8.0	-2.0	2.0	2.0	-2.0	2.0	2.0	0.0	0.0	556.	849.	3820.	15.7	11.35	12.71	-5.42
G7	-6.0	-2.0	2.0	2.0	0.0	-2.0	2.0	0.0	0.0	342.	916.	3970.	20.2	14.24	14.38	-5.60
G8	-6.0	-2.0	0.0	0.0	0.0	0.0	-2.0	0.0	0.0	934.	825.	5270.	18.4	13.10	13.10	-1.25
G9	-6.0	2.0	-2.0	0.0	-2.0	0.0	-2.0	0.0	0.0	278.	766.	3150.	11.5	12.20	7.00	1.65
H0	-6.0	2.0	2.0	0.0	0.0	0.0	-2.0	0.0	0.0	288.	752.	3700.	13.1	12.30	7.50	-2.72
H1	-8.0	-2.0	0.0	0.0	-2.0	2.0	0.0	0.0	0.0	664.	792.	4200.	14.3	10.49	12.04	-1.39
H2	-8.0	2.0	-2.0	2.0	2.0	0.0	0.0	0.0	0.0	1545.	946.	6830.	15.8	14.79	14.27	-0.74
H3	-6.0	2.0	2.0	-2.0	2.0	0.0	0.0	0.0	0.0	767.	785.	5300.	15.8	13.39	9.50	-1.66
H4	-8.0	-2.0	0.0	0.0	0.0	-2.0	0.0	0.0	0.0	786.	896.	3825.	18.5	12.57	15.73	-2.13
H5	-6.0	0.0	0.0	0.0	-2.0	0.0	2.0	0.0	0.0	332.	754.	4350.	12.1	11.79	8.53	-0.76
H6	-6.0	0.0	-2.0	2.0	-2.0	0.0	2.0	0.0	0.0	218.	768.	4070.	12.9	12.02	8.83	0.24
H7	-6.0	-2.0	0.0	2.0	-2.0	0.0	2.0	0.0	0.0	216.	788.	3400.	14.4	12.06	11.03	-2.49
H8	-6.0	2.0	0.0	2.0	0.0	-2.0	0.0	0.0	0.0	77.	772.	3170.	14.6	12.60	8.08	-1.91
H9	-6.0	0.0	0.0	2.0	0.0	0.0	-2.0	0.0	0.0	612.	789.	3950.	15.9	12.61	10.21	-2.12
I1	-6.0	-2.0	2.0	2.0	-2.0	2.0	2.0	0.0	0.0	445.	804.	3815.	14.8	12.21	10.87	-4.83
I2	0.0	-2.0	2.0	2.0	0.0	0.0	0.0	0.0	0.0	220.	759.	4080.	13.6	16.41	7.80	-3.62
I3	-6.0	-2.0	2.0	2.0	0.0	0.0	0.0	0.0	0.0	485.	852.	3890.	17.6	13.33	13.25	-5.04
I4	0.0	-2.0	2.0	2.0	-2.0	2.0	2.0	0.0	0.0	613.	756.	5150.	13.4	16.15	6.75	-3.46
I5	0.0	-2.0	2.0	0.0	-2.0	2.0	0.0	0.0	0.0	480.	739.	5000.	11.7	16.11	6.98	-2.34
I6	0.0	-2.0	0.0	2.0	0.0	0.0	2.0	0.0	0.0	392.	755.	3795.	13.4	16.54	8.29	-1.45
I7	-2.0	2.0	-2.0	0.0	0.0	2.0	2.0	0.0	0.0	720.	779.	7435.	15.8	15.90	5.62	2.48
I8	-4.0	0.0	-2.0	0.0	0.0	0.0	2.0	0.0	0.0	404.	756.	5095.	14.7	13.67	6.90	1.55
I9	-2.0	-2.0	0.0	-2.0	-2.0	2.0	0.0	0.0	0.0	296.	748.	3650.	12.9	14.62	8.74	0.53
J0	-4.0	-2.0	0.0	-2.0	-2.0	-2.0	0.0	0.0	0.0	296.	757.	3220.	12.7	13.16	9.95	0.26
J1	-2.0	-2.0	2.0	2.0	0.0	0.0	0.0	0.0	0.0	245.	773.	3740.	14.4	15.07	9.25	-3.88
J2	-4.0	0.0	0.0	-2.0	-2.0	0.0	0.0	0.0	0.0	255.	745.	4205.	14.0	13.40	7.80	0.61
J3	-2.0	-2.0	0.0	2.0	0.0	0.0	2.0	0.0	0.0	328.	769.	3380.	14.2	15.22	9.62	-1.75
J4	-6.0	-2.0	2.0	0.0	-2.0	2.0	0.0	0.0	0.0	531.	768.	4215.	12.5	11.75	10.49	-3.13
J5	-2.0	-2.0	-2.0	2.0	-2.0	0.0	2.0	0.0	0.0	295.	740.	4340.	12.2	14.60	8.46	0.68

TABLE 7 (Continued)

CASE NO	FLAP INPUTS -DEGREES									PYLON EXCITATION	HORSEPOWER	OP BENDING MOMENT	MAX LOCAL ANGLE OF ATTACK-DEG	PITCH HORN INPUT DEGREES		
	DO	D1S	D1C	D2S	D2C	D3S	D3C	D4S	D4C	+/- LBS		+/- IN-LBS		AO	B1S	A1S
J6	-2.0	-2.0	2.0	2.0	-2.0	2.0	2.0	0.0	0.0	480.	765.	4695.	13.6	14.71	8.00	-3.66
J8	-4.0	-2.0	2.0	2.0	0.0	2.0	2.0	0.0	0.0	635.	808.	4400.	15.0	14.18	10.93	-4.47
J9	-6.0	2.0	-2.0	2.0	-2.0	-2.0	2.0	0.0	0.0	412.	771.	5024.	12.8	12.02	6.73	0.46
K0	-4.0	-2.0	2.0	2.0	0.0	0.0	0.0	0.0	0.0	292.	791.	3520.	15.7	13.88	10.88	-4.30
K2	-4.0	-2.0	2.0	2.0	-2.0	2.0	2.0	0.0	0.0	412.	782.	4170.	14.0	13.40	9.38	-4.11
K3	-4.0	-2.0	0.0	2.0	0.0	0.0	2.0	0.0	0.0	414.	789.	3270.	15.2	14.09	11.24	-2.23
K4	-4.0	0.0	-2.0	2.0	-2.0	-2.0	2.0	0.0	0.0	380.	766.	4780.	12.8	13.37	7.74	0.52
K5	-6.0	0.0	2.0	-2.0	-2.0	0.0	-2.0	0.0	0.0	225.	753.	3210.	12.4	11.82	8.65	-1.85
K6	-4.0	0.0	2.0	0.0	-2.0	0.0	0.0	0.0	0.0	110.	739.	3805.	10.1	13.16	7.23	-2.53
K7	-6.0	2.0	2.0	-2.0	0.0	-2.0	0.0	0.0	0.0	237.	756.	3270.	12.8	12.34	7.78	-1.79
K9	-4.0	2.0	2.0	-2.0	0.0	-2.0	0.0	0.0	0.0	242.	743.	3825.	12.0	13.70	6.51	-1.41
L0	-4.0	2.0	0.0	0.0	0.0	-2.0	0.0	0.0	0.0	144.	746.	3505.	12.5	13.75	6.63	-0.35
L1	0.0	2.0	0.0	0.0	0.0	-2.0	0.0	0.0	0.0	289.	783.	4570.	11.0	17.08	4.10	0.25
L2	0.0	0.0	0.0	0.0	0.0	-2.0	0.0	0.0	0.0	204.	754.	3600.	10.8	16.64	6.28	-0.05
L3	-2.0	2.0	0.0	0.0	0.0	-2.0	0.0	0.0	0.0	217.	756.	3810.	11.3	15.32	5.37	-0.06
L4	-2.0	0.0	0.0	2.0	0.0	-2.0	0.0	0.0	0.0	116.	769.	3550.	14.0	15.21	7.62	-1.41
L8	-2.0	2.0	2.0	0.0	0.0	-2.0	0.0	0.0	0.0	212.	755.	4150.	11.3	15.19	5.00	-2.20
L9	-2.0	2.0	0.0	-2.0	0.0	-2.0	0.0	0.0	0.0	272.	766.	4575.	12.5	15.51	5.64	0.99
M0	-4.0	2.0	2.0	0.0	0.0	-2.0	0.0	0.0	0.0	147.	752.	3635.	12.3	13.67	6.38	-2.50
M1	-4.0	0.0	-2.0	-2.0	-2.0	0.0	0.0	0.0	0.0	373.	765.	5232.	15.2	13.71	8.21	2.83
M2	-4.0	-2.0	-2.0	0.0	-2.0	0.0	0.0	0.0	0.0	236.	749.	3415.	13.6	13.31	9.93	1.50
M3	-6.0	2.0	2.0	2.0	0.0	-2.0	0.0	0.0	0.0	127.	783.	3625.	15.1	12.58	7.97	-4.13
M4	-6.0	2.0	2.0	2.0	-2.0	-2.0	0.0	0.0	0.0	360.	778.	4700.	13.3	11.83	6.21	-3.85
M5	-6.0	0.0	2.0	2.0	-2.0	-2.0	0.0	0.0	0.0	317.	785.	3905.	14.5	11.81	8.54	-4.23
M6	-2.0	-2.0	0.0	0.0	-2.0	0.0	0.0	0.0	0.0	148.	738.	3545.	11.8	14.58	8.49	-0.39
M7	-2.0	-2.0	2.0	-2.0	-2.0	0.0	0.0	0.0	0.0	204.	740.	3995.	12.4	14.59	8.47	-1.52
M8	-2.0	-2.0	2.0	0.0	-2.0	0.0	0.0	0.0	0.0	126.	740.	3500.	10.4	14.48	8.23	-2.49
M9	-2.0	-2.0	0.0	-2.0	-2.0	0.0	0.0	0.0	0.0	257.	746.	4435.	14.0	14.75	8.78	0.60
N0	-4.0	2.0	2.0	2.0	0.0	-2.0	0.0	0.0	0.0	162.	769.	4190.	14.3	13.77	6.26	-3.65
N1	-4.0	0.0	2.0	2.0	0.0	-2.0	0.0	0.0	0.0	163.	784.	3680.	15.7	13.95	8.55	-4.06
N2	-4.0	-2.0	2.0	0.0	-2.0	0.0	0.0	0.0	0.0	132.	743.	3230.	10.8	13.03	9.29	-2.81
N3	-2.0	-2.0	2.0	2.0	-2.0	0.0	0.0	0.0	0.0	102.	754.	3810.	12.7	14.53	8.08	-3.63
N4	-2.0	0.0	2.0	0.0	-2.0	0.0	0.0	0.0	0.0	98.	745.	4155.	9.8	14.72	6.20	-2.24
N5	-6.0	-2.0	2.0	2.0	-2.0	0.0	0.0	0.0	0.0	109.	795.	2850.	14.4	11.93	10.86	-4.66
N6	-6.0	0.0	2.0	0.0	-2.0	0.0	0.0	0.0	0.0	150.	750.	3410.	10.8	11.75	8.45	-2.94
N7	-4.0	2.0	3.0	2.0	-2.0	0.0	0.0	0.0	0.0	69.	777.	3360.	14.0	13.12	9.32	-5.17
N8	-2.0	-2.0	0.0	2.0	-2.0	0.0	0.0	0.0	0.0	97.	745.	3550.	11.6	14.59	8.39	-1.42
N9	-6.0	-2.0	0.0	2.0	-2.0	0.0	0.0	0.0	0.0	149.	779.	2550.	13.5	11.89	10.92	-2.38
O0	-4.0	0.0	0.0	0.0	-2.0	0.0	0.0	0.0	0.0	152.	740.	3790.	11.8	13.32	7.63	-0.42
Z4	-4.0	-2.0	-2.0	0.0	-2.0	-2.0	2.0	0.0	0.0	343.	768.	4550.	13.4	13.26	10.03	1.36
Z5	-4.0	-2.0	-2.0	2.0	-2.0	0.0	0.0	0.0	0.0	144.	751.	3040.	11.7	13.25	9.75	0.33
Z6	-4.0	-2.0	0.0	0.0	-2.0	-2.0	2.0	0.0	0.0	371.	758.	4040.	12.1	13.05	9.62	-0.87
Z7	-4.0	-2.0	0.0	2.0	-2.0	0.0	0.0	0.0	0.0	94.	752.	3080.	12.3	13.08	9.41	-1.91

TABLE 8. MFS CONTROL STUDY, TRIMMED CASES WITH FOUR/REV PYLON EXCITATION LESS THAN OR EQUAL TO ±150 LB

F_z = 11500 lb
F_x = 907 lb
V = 120 kt

C_z/σ = .090
ΩR = 613 fps

δ_o = -2°					δ_o = -4°					δ_o = -6°				
Case No.	Pylon Load ±Lb	Bending Moment In.-Lb P/P	Rotor HP	Max. Local Angle Deg	Case No.	Pylon Load ±Lb	Bending Moment In.-Lb P/P	Rotor HP	Max. Local Angle Deg	Case No.	Pylon Load ±Lb	Bending Moment In.-Lb P/P	Rotor HP	Max. Local Angle
L4	116	7100	769	14.0	B9*	73	6440	764	13.2	H8	77	6340	772	14.6
M6*	148	7090	738	11.8	Z7*	94	6160	752	12.3	M3	127	7250	783	15.1
N3*	102	7620	754	12.7	K6*	110	7610	765	13.6	N6*	150	6830	750	10.8
N8*	97	7085	745	11.6	L0	144	7010	746	12.5	N9*	148	5100	779	13.5
N4*	98	8370	745	9.8	M0	147	7270	752	12.3	N5*	109	5700	795	14.4
					Z5*	144	6080	751	11.5					
					N2*	132	6460	743	10.8					
					N7*	69	6720	777	14.0					

* These cases have no third harmonic flap input.

TABLE 9. MFS CONTROL STUDY, SUMMARY OF OPTIMUM FLAP CONTROL REGION

$\delta_{3S} = \delta_{3C} = 0$

V = 120 kt F_z = 11500 lb F_x = 907 lb

CODE / CASE # / R_{vib} / BM / HP / α_{max}		$\delta_o = -2°$				$\delta_o = -4°$				$\delta_o = -6°$			
		δ_{2s} = 0°		δ_{1s} = 0°		δ_{1s} = -2°		δ_{1s} = 0°		δ_{1s} = -2°		δ_{1s} = 0°	
		δ_{2s}=0°	δ_{2s}=2°	δ_{2s}=0°	δ_{2s}=2°	δ_{2s}=0°	δ_{2s}=2°	δ_{2s}=0°	δ_{2s}=2°	δ_{2s}=0°	δ_{2s}=2°	δ_{2s}=0°	δ_{2s}=2°
δ_{1c} = -2°	δ_{2c} = -2°						Z5 144 6080 751 11.5						
δ_{1c} = 0°			N8 97 7085 745 11.6				Z7 94 6160 752 12.3	0Ø 152 7580 740 11.8			N9 148 5100 779 13.5		
δ_{1c} = +2°			N3 102 7620 754 12.7	N4 98 8370 745 9.8			B9 73 6440 764 13.2	K6 110 7610 765 13.6			N5 109 5700 745 14.4	N6 150 6830 750 10.8	
δ_{1c} = +3°							N7 69 6720 777 14.0						

TABLE 10. MULTICYCLIC FLAP SYSTEM, SURGEN MODEL 6 VS 6F AIRLOADS

	A0-Deg		B1S-Deg		A1S-Deg		4/Rev Pylon Load +/- Lb		Bending Moment +/- In -Lb	
Case	6F	SURGEN	6F	SURGEN	6F	SURGEN	6F	SURGEN	6F	SURGEN
K7	12.34	12.45	7.78	7.99	-1.79	-1.78	237	248	3270	3480
K9	13.70	13.75	6.51	6.64	-1.40	-1.42	242	196	3825	3700
L0	13.75	13.83	6.63	6.63	-0.35	-0.31	144	166	3505	3435
L1	17.08	17.03	4.10	3.93	0.25	0.23	289	277	4670	4650
L2	16.64	16.69	6.28	6.39	-0.05	-0.02	204	238	3600	4140
L3	15.32	15.33	5.37	5.22	-0.06	0	217	191	3810	3945
L4	15.21	15.18	7.62	7.96	-1.41	-1.49	116	189	3550	3525
L8	15.19	15.19	5.00	4.93	-2.20	-2.16	212	176	4150	3995
L9	15.51	15.50	5.64	5.67	0.99	1.02	272	223	4575	4335
M0	13.67	13.71	6.38	6.23	-2.50	-2.46	147	142	3635	3599
M1	13.71	13.75	8.21	7.69	2.83	2.92	373	183	5230	4510
M2	13.31	13.35	9.93	9.78	1.50	1.53	236	190	3415	3440
M3	12.58	12.59	7.97	7.75	-4.13	-4.11	127	135	3625	3650
M4	11.83	11.84	6.21	6.58	-3.85	-3.89	360	313	4700	4505
M5	11.81	11.85	8.54	8.76	-4.23	-4.25	317	126	3905	4005
M6	14.58	14.46	8.49	8.02	-0.39	-0.32	148	137	3545	3510
M7	14.59	14.47	8.47	7.85	-1.52	-1.49	204	135	3995	3535
M8	14.48	14.38	8.23	7.67	-2.49	-2.49	120	126	3535	3500
M9	14.75	14.66	8.78	8.17	0.60	0.68	257	149	4435	3820
N0	13.77	13.84	6.26	6.27	-3.65	-3.70	162	133	4190	3845
N1	13.95	13.91	8.95	8.79	-4.06	-4.03	163	148	3630	3575
N2	12.03	12.99	9.29	8.95	-2.81	-2.84	132	130	3230	3190

$C_z/\sigma = .090$

A review of the harmonic content of the blade root shears used to calculate the four/rev pylon excitation indicates that the largest component is contributed by the five/rev in-plane component. The final item to note is that for the cases with low pylon loading, the blade local angle of attack reached a peak in the .6 to .7 nondimensional blade station area. For the majority of cases the maximum angle occurs in the inboard region of the blade (.4) and is reduced toward the tip. This indicates that dual control inputs can produce the ideal torsional shape to reduce rotor parameters to levels not possible with the single input.

When it was found that a reduction in vibratory pylon loading could be obtained with only the addition of second harmonic, a cursory check was made of the combination of second and fourth harmonic on this parameter. Trim case B9 which had the minimum pylon loading ($\pm$73 lb) was repeated with four combinations of four/rev sine and cosine components. For these four cases investigated all of the rotor parameters exceeded the values obtained by the original case (Table 11).

In addition to C_z/σ of .090, 23 cases were trimmed at 12500 lb (C_z/σ = .098) of rotor lift. All of the cases at this load level had flap control inputs selected to correspond with cases at C_z/σ of .090 to permit direct comparison of the two load levels. Table 12 is a listing of the trimmed pitch horn control and rotor parameters at this disk loading. The first ten cases selected at the higher rotor loading were those with the lowest pylon loadings to date. All of the parameters except pylon excitation exhibited an increase; it displayed a random pattern of nonuniform increases and decreases. The remaining cases run were grouped at increased but similar pylon loads to ascertain if a trend could be noted at each level. The resultant pylon excitations were randomly scattered and indicated no discernible pattern.

A check of the cases at 12500 lb rotor lift (Z7, B9) that correspond to the optimum area at 11500 lb reveal that all rotor parameters are within the acceptable range defined for the CTR. Since no attempt was made to model and optimize the dependent variable at 12500 lb, the values shown may not be the minimum obtainable at this disk loading.

An attempt was made to expand the model by making gross weight a dependent variable. This effort was not successful because of the sparsity of data at various levels of gross weight.

TABLE 11. MFS CONTROL STUDY, EFFECT OF FOUR/REV FLAP INPUT ON ROTOR PARAMETERS

F_z = 11500 lb
F_x = 907 lb
V = 120 kt

C_z/σ = .090
ΩR = 613 fps

Flap Input - Deg												
δ_o	δ_{1s}	δ_{1c}	δ_{2s}	δ_{2c}	δ_{3s}	δ_{3c}	δ_{4s}	δ_{4c}	Pylon Excitation ±Lb	Horsepower	Bending Moment In -Lb p/p	Max. Blade Local Angle of Attack Deg
-4	-2	2	2	-2	0	0	0	0	73	764	6440	13.2
-4	-2	2	2	-2	0	0	+2	-2	404	798	7520	15.0
-4	-2	2	2	-2	0	0	-2	2	282	807	8900	13.8
-4	-2	2	2	-2	0	0	+2	0	280	775	6970	13.8
-4	-2	2	2	-2	0	0	-2	0	195	797	8240	14.4

TABLE 12. MFS CONTROL STUDY, SUMMARY OF TRIMMED CASES

F_z = 12500 lb C_z/σ = .098

V = 120 kt μ = .333

ΩR = 613 fps

Case No.	Flap Inputs - Degrees D0	D1S	D1C	D2S	D2C	D3S	D3C	Pylon Excitation +/- lb	HP	OP Bending Moment +/- in -lb	Max. Local Angle of Attack-Deg	Pitch Horn Input Degrees A0	B1S	A1S
E5	-4.0	-2.0	0.0	0.0	-2.0	-2.0	-2.0	283.	807.	2710.	15.0	14.25	10.36	-1.03
Z5	-4.0	-2.0	-2.0	2.0	-2.0	0.0	0.0	255.	787.	3260.	13.2	14.26	10.09	0.15
Z7	-4.0	-2.0	0.0	2.0	-2.0	0.0	0.0	189.	790.	3070.	14.0	14.16	9.88	-2.08
B9	-4.0	-2.0	2.0	2.0	-2.0	0.0	0.0	139.	813.	3370.	15.3	14.28	9.93	-4.36
A3	-2.0	0.0	0.0	-2.0	-2.0	0.0	0.0	256.	784.	5575.	15.1	15.90	6.85	1.01
K6	-4.0	0.0	2.0	0.0	-2.0	0.0	0.0	135.	760.	3920.	11.4	13.96	7.38	-2.64
L0	-4.0	2.0	0.0	0.0	0.0	-2.0	0.0	126.	780.	3820.	13.9	14.80	7.11	-0.46
L4	-2.0	0.0	0.0	2.0	0.0	-2.0	0.0	150.	814.	3730.	16.3	16.60	8.57	-1.75
M3	-6.0	2.0	2.0	2.0	0.0	-2.0	0.0	190.	840.	3695.	17.3	14.21	9.20	-4.51
H8	-6.0	2.0	0.0	2.0	0.0	-2.0	0.0	174.	824.	3215.	16.5	14.09	9.19	-2.19
M6	-2.0	-2.0	0.0	0.0	-2.0	0.0	0.0	177.	756.	3840.	13.4	15.37	8.57	-0.50
N2	-4.0	-2.0	2.0	0.0	-2.0	0.0	0.0	188.	767.	3365.	12.0	13.86	9.48	-2.97
N0	-4.0	2.0	2.0	2.0	0.0	-2.0	0.0	146.	807.	4360.	16.0	15.06	7.06	-3.93
I9	-2.0	-2.0	0.0	-2.0	-2.0	2.0	0.0	789.	807.	7410.	18.4	16.15	9.29	0.94
J0	-4.0	-2.0	0.0	-2.0	-2.0	-2.0	0.0	310.	794.	3970.	14.5	14.20	10.31	0.21
J5	-2.0	-2.0	-2.0	2.0	-2.0	0.0	2.0	304.	783.	4690.	13.8	15.70	8.90	0.54
M7	-2.0	-2.0	2.0	-2.0	-2.0	0.0	0.0	226.	757.	4360.	14.1	15.38	8.55	-1.57
L2	0.0	0.0	0.0	0.0	0.0	-2.0	0.0	150.	785.	4000.	12.7	17.52	6.43	-0.13
N1	-4.0	0.0	2.0	2.0	0.0	-2.0	0.0	231.	871.	3950.	18.9	15.93	10.62	-4.56
K4	-4.0	0.0	-2.0	2.0	-2.0	-2.0	2.0	257.	798.	4945.	14.4	14.45	8.19	0.30
A9	0.0	0.0	2.0	0.0	-2.0	-2.0	0.0	381.	797.	4975.	10.8	17.04	4.78	-2.18
M1	-4.0	0.0	-2.0	-2.0	-2.0	0.0	0.0	594.	820.	6995.	17.5	15.00	8.71	2.94
I5	0.0	-2.0	2.0	0.0	-2.0	2.0	0.0	491.	761.	5215.	13.8	16.89	7.05	-2.38

CONCLUSIONS

For the limited scope of this study which was restricted to a four bladed dual control rotor at one gross weight (11500 lb) and one forward speed (120 knots):

1. The addition of second harmonic flap input reduced the four/rev pylon excitation loads 40 percent.

2. Third and fourth harmonic flap inputs appear to negate gains produced by second harmonic input.

3. In general, five/rev in-plane root shears produce the largest component of pylon excitation.

4. Results of modeling of rotor parameters and pitch horn controls produce excellent trends and good correlation with only a small percentage of cases trimmed.

RECOMMENDATIONS

This study should be expanded to ascertain the effects of the following:

1. Analytical

    a. Gross Weight
    b. Four/Rev
    c. Advance Ratio
    d. Number of Blades
    e. Can Models be Expanded to Include Gross Weight and Advance Ratio

2. Test Verification of Analytical Results

REFERENCES

1. McCloud, John L., III, AN ANALYTICAL STUDY OF A MULTICYCLIC CONTROLLABLE TWIST ROTOR, AHS Preprint No. 932, American Helicopter Society Annual National Forum, May, 1975.

2. Lemnios, A. Z. and Smith, A. F., AN ANALYTICAL EVALUATION OF THE CONTROLLABLE TWIST ROTOR PERFORMANCE AND DYNAMIC BEHAVIOR, USAAMRDL Technical Report 72-16, U. S. Army Air Mobility Research and Development Laboratory, Eustis Directorate, Fort Eustis, Virginia, May 1972.

3. McCloud, John L. III, STUIDES OF A LARGE-SCALE JET-FLAP ROTOR IN THE 40- BY 80-FOOT WIND TUNNEL, Paper presented at the Mideast Region Symposium of American Helicopter Society, October 1972.

4. McCloud, John L., III, and Kretz, M., MULTICYCLIC JET-FLAP CONTROL FOR ALLEVIATION OF HELICOPTER BLADE STRESSES AND FUSELAGE VIBRATION, Specialist Meeting on Rotorcraft Dynamics, NASA SP 352, February, 1974.

5. Lemnios, A. Z., ROTARY WING DESIGN METHODOLOGY, Paper presented at the AGARD Specialists Meeting on Helicopter Rotor Loads Prediction Methods, March 1973.

APPENDIX A

LISTING AND EXAMPLE RUN OF BASIC PROGRAM TO CALCULATE ROTOR PYLON EXCITING LOAD "SHEAR"

MFS STUDY

CALCULATION OF PYLON EXCITATION FORCES

RUN
SHEAR8 CASE Z7 F_z = 11500 LB, V = 120 KT

PROGRAM "SHEAR8" - RP 075E
RESOLVES BLADE ROOT SHEARS INTO PYLON EXCITATION FORCES

CASE IDENT ? 73001 Z7

DO YOU WISH TO TABULATE RESPONSES (Y OR N) ?Y
NUMBER OF BLADES ?4
INPUT COEFFICIENTS AS FOLLOWS :
VERTICAL 4 P REAL ?3
IMAG ?-12
IN-PLANE 3 P REAL ?-16
IMAG ?-2
5 P REAL ?24
IMAG ?-2

PHASE	VERT	F & A	LAT	RESULT
15	-.832193	-20.7055	13.3843	24.6688
30	-13.6077	-40.	9.85641	43.3857
45	-25.4558	-56.5685	5.65686	62.2896
60	-35.5692	-69.282	1.07181	77.8866
75	-43.2586	-77.274	-3.58629	-88.631
90	-48	-80.	-7.99998	-93.6376
105	-49.4703	-77.2741	-11.8685	-92.5173
120	-47.5692	-69.2821	-14.9282	-85.3563
135	-42.4265	-56.5686	-16.9706	-72.7188
150	-34.3924	-40.0001	-17.8564	-55.6929
165	-24.0145	-20.7057	-17.5254	-36.2293
180	-12.0001	-1.79763E-04	-16.	-20.0001
195	.832063	20.7053	-13.3843	-24.6687
210	13.6076	39.9998	-9.85645	-43.3855
225	25.4558	56.5684	-5.65689	-62.2895
240	35.5691	69.2819	-1.07186	-77.8864
255	43.2585	77.274	3.58624	88.6309
270	48.	80.	7.99994	93.6376
285	49.4703	77.2741	11.8685	92.5173
300	47.5693	69.2822	14.9282	85.3564
315	42.4265	56.5688	16.9705	72.7189
330	34.3924	40.0003	17.8564	55.693
345	24.0146	20.7059	17.5254	36.2294
360	12.0002	3.59527E-04	16.	20.0002

HUB VIBRATORY 4 PER REV SHEARS

MAX RESULTANT = + OR - 93.6376
MAX VERT = + OR - 49.4703
MAX F & A = + OR - 80.
MAX LAT = + OR - 17.8564
IN PLANE RESULT = + OR - 80.399

APPENDIX B

FORTRAN LISTING OF SURGEN

This program for use of IBM 360/40. "MODEL" is the form of Equation (4).

```
OIS FORTRAN IV 360N-FO-479 3-6          MAINPGM          DATE   04/06/76      TIME     11.15.43

0001              REAL MI
0002              DIMENSION Z(200,15),F(200,45),X(45),Y(44),
                 1 Q(44,44), P(44,44),G(44),B(44),ANS1(44)
                 2,ZORIG(200,15)
                 3,HEAD(20),TITLES(15,5)
0003              5 FORMAT(1H1,////,10X,'SUBGEN**** GENERATES A RESPONSE MATRIX TO FIT
                  1 A SET OF DATA POINTS'///)
                C
0004              READ(1,505) HEAD
0005            505 FORMAT(20A4)
0006              READ(1,10) NDATPT,NCOLS,NVAR,ILEFT,NMOD
0007              READ(1,510)(((TITLES(I,J),J=1,5),I=1,ILEFT)
                C
                C
                C     NDATPT = NO OF DATA POINTS (CASES)
                C       NO OF COLUMNS TO BE READ
                C       NVAR = NO OF VARIABLES TO BE FIT
                C      ILEFT = NO OF ITEMS TO BE MODELLED
                C
                C
0008            510 FORMAT(8(5A2))
0009              NCTL=7
0010              IF( NMOD .EQ. 2) NCTL=9
                C
                C     NMOD = 1
                C       MODEL1 = MULTICYCLIC CONTROL THRU THIRD HARMONIC
                C         NMOD = 2
                C     MODEL2 = CTR DO,DIS,DIC
                C
0011             10 FORMAT(8I10)
0012              INDEX=1
0013              KOUNT=0
0014              DO 20 I=1,NDATPT
0015             20 READ(1,30) (Z(I,J),J=1,NCOLS)
0016             30 FORMAT(8F10.2)
0017              DO 25 I=1,NDATPT
0018              DO 25 J=1,NCOLS
0019             25 ZORIG(I,J)=Z(I,J)
0020              Z1=NDATPT
0021              Z2=NCOLS
0022              N=NVAR
0023              N1=NVAR+1
0024              N2=NVAR+2
0025             35 DO 31 I=1,NDATPT
0026              DO 31 J=1,N2
0027             31 F(I,J)=1.0
0028               WRITE(3,5)
0029              WRITE(3,516)
0030            516 FORMAT(//)
0031              WRITE(3,505) HEAD
0032              GO TO (40,45),NMOD
0033             40 CALL MODEL1(F,ZORIG,NDATPT,INDEX)
0034              GO TO 46
0035             45 CALL MODEL2(F,ZORIG,NDATPT,INDEX)
```

```
OS FORTRAN IV G1JN-F0-479 3-6          MAINOGM              DATE   04/06/76      TIME     13.15.48

0093          175 FORMAT(1H ,37X,'EST VALUE',4X,'DIFFERENCE',4X,'PERCENT',4X,'DO',
                 10X,'D1S',6X,'D1C'/)
0094              GO TO 187
0095          181 WRITE(3,185)
0096          185 FORMAT(1H ,37X,'EST VALUE',4X,'DIFFERENCE',4X,'PERCENT',4X,'DO',
                 10X,'D1S',6X,'D1C',5X,'D2S',5X,'D2C',5X,'D3S',5X,'D3C'/)
0097          187 T2=0.0
0098              DO 180 J=1,NDATPT
0099               S8=0.0
0100              DO 190 I=1,N1
0101          190 S8=S8+F(J,I)*B(I)
0102              T2=T2+(F(J,N2)-S7/Z1)**2
0103              S0=S8-F(J,N2)
0104              Z0=S0*100./F(J,N2)
0105              WRITE(3,200) J,F(J,N2),S8,S0,Z0,(ZORIG(J,JJ),JJ=1,NCTL)
0106          180 Z(J,1)=S0
0107          200 FORMAT(I10,F20.3,2F15.3,F12.3,7F8.2/)
0108          210 FORMAT(/////,20X,'ANALYSIS OF RESIDUALS')
0109              NZERO=NDATPT-1
0110              DO 250 I=1,NZERO
0111              M=I
0112              MM=I+1
0113              DO 260 J=MM,NDATPT
0114              IF(Z(M,1)-Z(J,1)) 260,260,270
0115          270 M=J
0116          260 CONTINUE
0117              IF(M .EQ. I) GO TO 250
0118               PT=Z(M,1)
0119              Z(M,1)=Z(I,1)
0120              Z(I,1)=PT
0121          250 CONTINUE
0122               S=0.0
0123              S2=0.0
0124              DO 280 I=1,NDATPT
0125              S=S+Z(I,1)
0126          280 S2=S2+Z(I,1)**2
0127              MI=S/Z1
0128              V=(Z1*S2-S*S)/(Z1*(Z1-1.))
0129              D=SQRT(V)
0130              WRITE(3,300) S,S2,MI,V,D
0131          300 FORMAT(20X,'SUM=',F15.4/9X,'SUM OF SQUARES=',F15.4/13X,'MEAN VALUE='
                 1 F15.4,/,15X,'VARIANCE=',F15.4/,5X,'STANDARD DEVIATION=' F15.4/)
0132              DU=SQRT((MI/B(1))**2)
0133              IF(DU-.01) 350,360,360
0134          360 B(1)=B(1)-MI
0135               CONST1=CONST1-MI
0136              GO TO 145
0137          350 R=SQRT(1.-S2/T2)
0138          370 FORMAT(5X,'MULT CORR COEFF=',F6.3/)
0139              WRITE(3,370) R
0140              WRITE(3,380)
0141              DO 400 I=1,NDATPT
0142              RRR=I
0143              ZEND=(RRR-.5)*100./Z1
0144          400 WRITE(3,410) Z(I,1),ZEND
0145          410 FORMAT(2F15.3)
0146              IF(KOUNT-ILEFT) 35,420,420
0147          380 FORMAT(20X,'CUMULATIVE DISTRIBUTION'/10X,'X',10X,'CUM PERCENT'
                 1 /21X,'OF POPULATION'/)
0148          420 CALL EXIT
0149              END
```

```
035 FORTRAN IV 360N-FO-479 3-6          MAINPGM          DATE   04/06/76      TIME     13.15.48

0036          46 KOUNT=KOUNT+1
0037             DO 32 I=1,N1
0038             DO 32 J=1,N1
0039             Q(I,J)=0.0
0040          32 P(I,J)=0.0
0041             DO 34 I=1,N1
0042             Y(I)=0.0
0043          34 B(I)=0.0
0044              DO 36 I=1,N2
0045          36 X(I)=1.0
0046              DO 55 I=1,NDATPT
0047              DO 55 J=1,NCOLS
0048          55 Z(I,J)=ZORIG(I,J)
0049             S5=0.0
0050             S6=0.0
0051             S7=0.0
0052             DO 60 L=1,NDATPT
0053             DO 70 I=2,N2
0054          70 X(I)=F(L,I)
0055             DO 80 I=1,N1
0056             DO 90 J=1,N1
0057          90 P(I,J)=P(I,J)+X(I)*X(J)
0058          80 Y(I)=Y(I)+X(I)*X(N2)
0059             S7=S7+X(N2)
0060          60 S5=S5+X(N2)*X(N2)
0061             M1=P(1,1)
0062             S2=Y(1)
0063             DO 100 I=2,N1
0064             II=I-1
0065             S1=P(1,I)
0066             S3=Y(I)
0067             S4=P(I,I)
0068             A=M1*S3-S1*S2
0069             BB=(M1*S4-S1*S1)*(M1*S5-S2*S2)
0070             RATIO=A/SQRT(BB)
0071             ROUND=     ((RATIO*1000.+.5)/1000.)
0072             WRITE(3,110) II,ROUND
0073         110 FORMAT(5X,'FACTOR',I3,5X,'CORRELATION=',F6.3)
0074         100 G(II)=A
0075             CALL MATINV(P,Q,C,NG,N1)
0076             CALL MTRXMP(N1,N1,1,Q,Y,R,0)
0077             WRITE(3,120)
0078         120 FORMAT(/,20X,'COEFFICIENTS OF BEST LINEAR FIT'/)
0079             DO 130 I=2,N1
0080         130 ANS1(I)=     ((B(I)*1000.+.5)/1000.)
0081             WRITE(3,140) (ANS1(I),I=2,N1)
0082         140 FORMAT(4(9F14.4/))
0083             CONST1=     ((B(1)*1000.+.5)/1000.)
0084         145 WRITE(3,150) CONST1
0085         150 FORMAT(10X,'CONSTANT TERM=',F10.4//)
0086             WRITE(3,160) (TITLES(KOUNT,J),J=1,5)
0087         160 FORMAT(20X,'TABLE OF RESIDUALS'/,5X,'POINT NO',7X,5A2)
0088             GO TO(181,170),NNOO
0089         170 WRITE(3,175)
```

```
DOS FORTRAN IV 360N-FO-479 3-6          MATINV              DATE    04/06/76      TIME     13.17.36

0001                SUBROUTINE MATINV (A,B,C,NG,NRA)
0002                DIMENSION A(44,44),IROW(44),ICOL(44),B(44,44),C(44,44),F(44)
0003                NG=0
0004                N=NRA
0005                M=N+1
0006                DO 7 I=1,N
0007                IROW(I)=I
0008                ICOL(I)=I
0009                DO 7 J=1,N
0010              7 B(I,J)=A(I,J)
0011                DO 20 K=1,N
0012                AMAX=B(K,K)
0013                DO 10 I=K,N
0014                DO 10 J=K,N
0015                IF(ABS(B(I,J))-ABS(AMAX))10,9,9
0016              9 AMAX=B(I,J)
0017                IC=I
0018                JC=J
0019             10 CONTINUE
0020                KI=ICOL(K)
0021                ICOL(K)=ICOL(IC)
0022                ICOL(IC)=KI
0023                KI = IROW(K)
0024                IROW(K)=IROW(JC)
0025                IROW(JC)=KI
0026                IF(AMAX)11,12,11
0027             12 NG=9
0028                GO TO 30
0029             11 DO 14 J=1,N
0030                E=B(K,J)
0031                B(K,J)=B(IC,J)
0032             14 B(IC,J)=E
0033                DO 15 I=1,N
0034                E=B(I,K)
0035                B(I,K)=B(I,JC)
0036             15 B(I,JC)=E
0037                DO 16 I=1,N
0038                IF(I-K)18,17,18
0039             17 F(I)=1
0040                GO TO 16
0041             18 F(I)=0
0042             16 CONTINUE
0043                PVT=B(K,K)
0044                DO 8 J=1,N
0045              8 B(K,J)=B(K,J)/PVT
0046                F(K)=F(K)/PVT
0047                DO 19 I=1,N
0048                IF(I-K)21,19,21
0049             21 AMULT=B(I,K)
0050                DO 22 J=1,N
0051             22 B(I,J)=B(I,J)-AMULT*B(K,J)
0052                F(I)=F(I)-AMULT*F(K)
0053             19 CONTINUE
0054                DO 20 I=1,N
0055             20 B(I,K)=F(I)
0056                DO 25 I=1,N
0057                DO 24 L=1,N
0058                IF(IROW(I)-L)24,23,24
0059             24 CONTINUE
0060             23 DO 25 J=1,N
0061             25 C(L,J)=B(I,J)
0062                DO 26 J=1,N
0063                DO 29 L=1,N
0064                IF(ICOL(J)-L)28,29,28
0065             28 CONTINUE
0066             29 DO 26 I=1,N
0067             26 B(I,L)=C(I,J)
0068             30 RETURN
0069                END
```

```
DEC FORTRAN IV 360N-FO-479 3-6          MODEL1          DATE   04/06/76     TIME    13.18.58

0001              SUBROUTINE MODEL1(F,Z,NDATPT,INDEX)
0002              DIMENSION F(200,45),Z(200,15)
0003              GO TO(1,2),INDEX
0004            1 K=0
0005            2 DO 10 I=1,NDATPT
0006              F(I,2)=Z(I,1)
0007              F(I,3)=Z(I,2)
0008              F(I,4)=Z(I,3)
0009              F(I,5)=Z(I,4)
0010              F(I,6)=Z(I,5)
0011              F(I,7)=Z(I,6)
0012              F(I,8)=Z(I,7)
0013              F(I,9)=Z(I,1)**2
0014              F(I,10)=Z(I,1)*Z(I,2)
0015              F(I,11)=Z(I,1)*Z(I,3)
0016               F(I,12)=Z(I,1)*Z(I,4)
0017              F(I,13)=Z(I,1)*Z(I,5)
0018              F(I,14)=Z(I,1)*Z(I,6)
0019              F(I,15)=Z(I,1)*Z(I,7)
0020              F(I,16)=Z(I,2)**2
0021              F(I,17)=Z(I,2)*Z(I,3)
0022              F(I,18)=Z(I,2)*Z(I,4)
0023              F(I,19)=Z(I,2)*Z(I,5)
0024              F(I,20)=Z(I,2)*Z(I,6)
0025              F(I,21)=Z(I,2)*Z(I,7)
0026              F(I,22)=Z(I,3)**2
0027              F(I,23)=Z(I,3)*Z(I,4)
0028              F(I,24)=Z(I,3)*Z(I,5)
0029              F(I,25)=Z(I,3)*Z(I,6)
0030              F(I,26)=Z(I,3)*Z(I,7)
0031              F(I,27)=Z(I,4)**2
0032              F(I,28)=Z(I,4)*Z(I,5)
0033              F(I,29)=Z(I,4)*Z(I,6)
0034              F(I,30)=Z(I,4)*Z(I,7)
0035              F(I,31)=Z(I,5)**2
0036              F(I,32)=Z(I,5)*Z(I,6)
0037              F(I,33)=Z(I,5)*Z(I,7)
0038              F(I,34)=Z(I,6)**2
0039              F(I,35)=Z(I,6)*Z(I,7)
0040              F(I,36)=Z(I,7)**2
0041              F(I,37)=Z(I,15)/10000.
0042              F(I,38)=Z(I,15)*Z(I,1)/10000.
0043              F(I,39)=Z(I,15)*Z(I,2)/10000.
0044              F(I,40)=Z(I,15)*Z(I,3)/10000.
0045              F(I,41)=Z(I,15)*Z(I,4)/10000.
0046              F(I,42)=Z(I,15)*Z(I,5)/10000.
0047              F(I,43)=Z(I,15)*Z(I,6)/10000.
0048           10 F(I,44)=Z(I,15)*Z(I,7)/10000.
0049              INDEX=2
0050              K=K+1
                C     SEVEN IS THE NO. OF CONTROLS OF SERVO FLAP
0051              N=K+7
0052              DO 20 I=1,NDATPT
0053           20 F(I,45)=Z(I,N)
0054              RETURN
0055              END
```

```
DOS FORTRAN IV 360N-FO-479 3-6          MODEL2              DATE    04/06/76      TIME     13.21.10

0001                SUBROUTINE MODEL2(F,Z,NDATPT,INDEX)
0002                DIMENSION F(200,45),Z(200,15)
0003                GO TO(1,2),INDEX
0004              1 K=0
0005              2 DO 10 I=1,NDATPT
0006                F(I,2)=Z(I,1)
0007                F(I,3)=Z(I,2)
0008                F(I,4)=Z(I,3)
0009                F(I,5)=Z(I,8)
0010                F(I,6)=Z(I,1)**2
0011                F(I,7)=Z(I,2)**2
0012                F(I,8)=Z(I,3)**2
0013                F(I,9)=Z(I,8)**2
0014                F(I,10)=Z(I,1)*Z(I,2)
0015                F(I,11)=Z(I,1)*Z(I,3)
0016                 F(I,12)=Z(I,2)*Z(I,3)
0017             10 F(I,13)=Z(I,1)*Z(I,2)*Z(I,3)
0018                INDEX=2
0019                K=K+1
                 C      THREE IS THE NO. OF CONTROLS OF SERVO FLAP
0020                N=K+3
0021                DO 20 I=1,NDATPT
0022             20 F(I,14)=Z(I,N)
0023                RETURN
0024                END
```



```
DOS FORTRAN IV 360N-FO-479 3-6          MTRXMP              DATE    04/06/76      TIME     13.24.12

0001                SUBROUTINE MTRXMP(NRA,NCA,NCB,A,B,C,NDIAG)
0002                DIMENSION A(44,44),B(44,1),C(44,1)
0003                IF(NDIAG)100,120,140
0004             100 DO 110 I=1,NRA
0005                DO 110 J=1,NCA
0006             110 A(I,J)=-A(I,J)
0007                RETURN
0008             120 DO 130 I=1,NRA
0009                DO 130 J=1,NCB
0010                C(I,J)=0
0011                DO 130 K=1,NCA
0012             130 C(I,J)=C(I,J)+A(I,K)*B(K,J)
0013                RETURN
0014             140 DO 150 I=1,NRA
0015                DO 150 J=1,NCB
0016             150 C(I,J)=A(I,I)*B(I,J)
0017                RETURN
0018                END
```

APPENDIX C

REPRESENTATIVE VARIABLE INFLOW, $C_z/\sigma = .098$

TABLE VIII. VARIABLE INFLOW $C_z/\sigma = .098$
LAMBDA X 100 *

PSI	RADIAL STATION 12.00	53.60	67.20	100.80	134.40	168.00	201.60	235.20	252.20	275.00	280.00	304.50	309.50	319.20	325.92	336.00
0	-3.22	-3.97	-4.15	-4.43	-2.35	-1.80	-1.40	-3.06	-6.18	-5.39	-5.18	-3.86	-3.72	-3.45	-3.31	-3.17
15	-2.10	-2.36	-2.45	-2.90	-2.08	-2.49	-6.87	-6.77	-7.58	-8.52	-8.58	-8.55	-8.52	-8.42	-8.35	-8.25
[illegible]	-2.39	-3.21	-3.36	-3.36	-10.34	-8.49	-7.50	-6.98	-6.81	-6.64	-6.62	-6.50	-6.49	-6.47	-6.46	-6.46
[illegible]	-5.31	-3.83	-2.96	-5.39	-7.10	-6.29	-5.94	-5.78	-5.74	-5.72	-5.72	-5.75	-5.76	-5.79	-5.82	-5.88
60	-4.44	-1.97	-5.60	-6.91	-6.07	-5.71	-5.51	-5.36	-5.29	-5.22	-5.21	-5.21	-5.22	-5.28	-5.33	-5.45
75	-5.35	-7.17	-6.92	-5.61	-5.13	-4.90	-4.85	-4.94	-4.97	-4.85	-4.81	-4.44	-4.42	-4.43	-4.40	-3.81
[illegible]	-2.07	-6.10	-5.51	-5.02	-4.91	-4.90	-4.69	-4.12	-4.04	-4.30	-4.35	-3.32	-2.86	-1.88	-1.79	-1.86
105	-2.46	-5.29	-5.09	-4.94	-4.74	-4.20	-3.95	-4.27	-4.46	-3.22	-2.86	-2.16	-2.21	-2.37	-2.46	-2.57
120	-5.91	-4.96	-4.88	-4.54	-4.01	-3.97	-4.28	-4.18	-2.88	-2.35	-2.38	-2.68	-2.71	-2.78	-2.82	-2.88
135	-5.27	-4.57	-4.42	-3.99	-3.98	-4.23	-4.38	-2.65	-2.52	-2.73	-2.76	-2.83	-2.94	-2.98	-3.00	-3.02
150	-4.49	-4.06	-3.99	-3.97	-4.16	-4.39	-3.30	-2.68	-2.81	-2.95	-2.97	-3.06	-3.06	-3.08	-3.09	-3.10
165	-3.64	-3.93	-3.91	-4.08	-4.30	-3.95	-2.78	-2.89	-2.99	-3.08	-3.09	-3.13	-3.13	-3.14	-3.15	-3.15
180	-2.72	-3.81	-3.97	-4.18	-4.25	-3.34	-2.87	-3.03	-3.10	-3.16	-3.16	-3.18	-3.18	-3.18	-3.18	-3.19
195	-1.70	-3.87	-4.04	-4.20	-3.94	-3.06	-2.97	-3.12	-3.18	-3.21	-3.22	-3.21	-3.21	-3.21	-3.20	-3.20
210	-2.48	-3.95	-4.06	-4.10	-3.67	-3.06	-3.04	-3.18	-3.22	-3.25	-3.25	-3.24	-3.23	-3.22	-3.21	-3.20
225	-5.95	-4.13	-4.01	-3.93	-3.53	-3.09	-3.08	-3.19	-3.24	-3.27	-3.27	-3.25	-3.24	-3.23	-3.22	-3.20
240	-5.28	-4.50	-3.89	-3.76	-3.69	-3.17	-3.08	-3.17	-3.22	-3.26	-3.26	-3.24	-3.24	-3.22	-3.20	-3.18
255	-4.35	-4.70	-3.73	-3.59	-3.51	-3.32	-3.13	-3.10	-3.14	-3.19	-3.19	-3.19	-3.19	-3.17	-3.16	-3.14
270	-3.49	-4.37	-3.64	-3.38	-3.52	-3.54	-3.40	-3.20	-3.11	-3.06	-3.06	-3.05	-3.05	-3.04	-3.03	-3.02
285	-2.69	-3.83	-3.59	-3.04	-3.44	-3.68	-3.83	-3.87	-3.82	-3.61	-3.57	-3.18	-3.13	-2.98	-2.90	-2.81
300	-1.33	-3.26	-3.39	-2.30	-3.16	-3.59	-3.85	-4.02	-4.09	-4.18	-4.19	-4.26	-4.26	-4.27	-4.26	-4.24
315	-3.27	-2.63	-2.93	0.10	-2.44	-3.21	-3.54	-3.71	-3.77	-3.83	-3.84	-3.91	-3.91	-3.93	-3.94	-3.95
330	-5.27	-1.77	-2.90	-9.63	-2.35	-2.23	-2.90	-3.17	-3.26	-3.38	-3.40	-3.57	-3.60	-3.68	-3.73	-3.82
345	-4.31	-3.88	-2.09	-4.83	-4.52	-4.47	-2.03	-1.83	-1.91	-2.04	-2.06	-2.43	-2.49	-2.67	-2.78	-2.92

* LAMBDA IS REFERENCED TO SHAFT PLANE AND IS POSITIVE UP THROUGH ROTOR
CHECK POINT 1 TAKEN.

APPENDIX D

BASIC LISTING OF MODEL4

This program was used to test all flap input combinatins used in our study. Only those control settings that met our criteria are printed for further consideration.

MODEL USED TO DEFINE CONTROL INPUTS FOR VIBRATORY HUB SHEARS

```
5     READ A0, A1, A2, A3, A4, A5, A6, A7, A8, A9
6     READ B0, B1, B2, B3, B4, B5, B6, B7, B8, B9
7     READ C0, C1, C2, C3, C4, C5, C6, C7, C8, C9
8     READ D0, D1, D2, D3, D4, D5
10    FOR I=0 TO -6 STEP -2
20    FOR J=2 TO -2 STEP -2
30    FOR K=2 TO -2 STEP -2
35    FOR L=2 TO -2 STEP -2
40    FOR M=2 TO -2 STEP -2
50    FOR M=2 TO -2 STEP -2
60    FOR O=2 TO -2 STEP -2
70    Z=A0+A1*I+A2*J+A3*K+A4*L+A5*M+A6*N+A7*O+A8*I*I+A9*I*J+B0*I*K
80    Z=Z+B1*I*L+B2*I*M+B3*I*N+B4*I*O+B5*J*J+B6*J*K+B7*J*L+B8*J*M
90    Z=Z+B9*J*N+C0*J*O+C1*K*K+C2*K*L+C3*K*M+C4*K*N+C5*K*O+O6*L*L
100   Z=Z+C7*L*M+C8*L*N+C9*L*O+D0*M*M+D1*M*N+D2*M*O+D3*N*N+D4*N*O+D5*O*O
105   IF Z>200 THEN 130
110   PRINT USING 120; I, J, K, L, M, N, O, Z
120   IMAGE 7(2D, 2X), 40, 20
130   NEXT O
132   NEXT N
134   NEXT M
136   NEXT L
138   NEXT K
140   NEXT J
142   NEXT I
150   PRINT LIN(2)
160   GOTO 5
459   REM ROOT SHEAR
460   DATA 410,52,34,11,52.35,-5.79,25.77,8.03,53.59,-6.14,5.5,8.75)
470   DATA 6.07,7.06,-7.71,-1.714,-2.927,-7.27,7.18,-3.31,5.35     )
480   DATA 11.04,3.09,-6.48,10.76,-13.4,-1.93,9.28,1.49,-1.8       )
490   DATA 13.17,-18.71,-13.29,-.56,3.48,40.78,-11.26,21.03        )
```

Coeff as calculated by SURGEN

Note in Statement 105, hub shears are limited to values below 200 lb, i.e., only those control inputs yielding shears in this range are printed out.

LIST OF SYMBOLS

a	generalized coefficient
A0	collective pitch horn input, deg
A1S	lateral pitch horn control input, deg
B1S	longitudinal pitch horn control input, deg
BM	out-of-plane bending moment
C_x	fore and aft rotor force coefficient, positive forward
C_z	vertical rotor force coefficient, positive up
CTR	Controllable Twist Rotor
F_x	fore and aft rotor force, lb
F_y	lateral rotor force, lb
F_z	vertical rotor force, lb
GW	helicopter gross weight, lb
HP	rotor horsepower
MFS	Multicyclic Flap System
q	bending displacement, in.
R	rotor radius, ft
r	distance from rotor hub to a blade station, ft
R_{vib}	vibratory pylon exciting load, lb
V	airspeed, kt
Y	any of the five rotor parameters of the MFS study
α	angle of attack of blade element, deg
α_{max}	maximum blade section angle of attack, deg
β	flapping response measured up from shaft plane, deg
δ	total flap deflection

LIST OF SYMBOLS (Continued)

δ_o	zero position for the flap, deg
δ_{ns}, δ_{nc}	sine and cosine n-th harmonic flap control input, deg
ζ	lag angle, deg
η_c	number of iterations to converge in aeroelastic trim program
θ	blade feathering displacement, deg
θ_{tw}	blade elastic twist displacement, deg
θ_x	built-in blade twist, deg
λ	inflow - ratio
μ	advance ratio
σ	rotor solidity
ψ	blade azimuth position, deg
Ω	rotor rotational speed, rad/sec
ΩR	rotor tip speed, ft/sec